AD-A128 743   IN-PLANE ACCELERATIONS AND FORCES ON FREQUENCY CHANGES   1/1
              IN DOUBLY-ROTATED..(U) PRINCETON UNIV NJ DEPT OF CIVIL
              ENGINEERING   P C LEE ET AL. APR 83 RR-83-SM-6
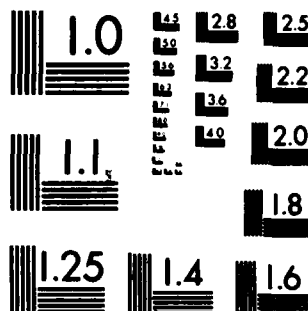UNCLASSIFIED  ARO-15648.6-EL DAAG29-79-C-0019        F/G 9/1       NL

END
DATE
FILMED

DTIC

MICROCOPY RESOLUTION TEST CHART
NATIONAL BUREAU OF STANDARDS-1963-A

AD A128743

IN-PLANE ACCELERATIONS AND FORCES ON

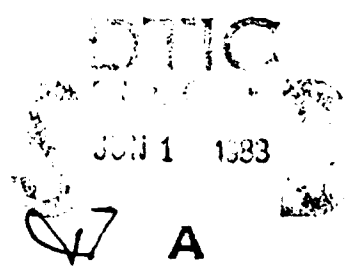FREQUENCY CHANGES IN

DOUBLY-ROTATED QUARTZ PLATES

FINAL REPORT
February 1979 – January 1983

P. C. Y. Lee and Kuang-Ming Wu

April 1983

U.S. Army Research Office
DAAG29-79-C-0019

**PRINCETON UNIVERSITY**

*Department of Civil Engineering*

**STRUCTURES AND MECHANICS**

| REPORT DOCUMENTATION PAGE | | READ INSTRUCTIONS BEFORE COMPLETING FORM |
|---|---|---|
| 1. REPORT NUMBER<br>Research Report 83-SM-6 | 2. GOVT ACCESSION NO.<br>AD A128 743 | 3. RECIPIENT'S CATALOG NUMBER |
| 4. TITLE (and Subtitle)<br><br>In-plane Accelerations and Forces on Frequency Changes in Doubly-Rotated Quartz Plates | | 5. TYPE OF REPORT & PERIOD COVERED<br>Final Report<br>Feb. 1, 1979-Jan. 31, 1983 |
| | | 6. PERFORMING ORG. REPORT NUMBER |
| 7. AUTHOR(s)<br>    P. C. Y. Lee   and   K. M. Wu | | 8. CONTRACT OR GRANT NUMBER(s)<br><br>DAAG29-79-C-0019 |
| 9. PERFORMING ORGANIZATION NAME AND ADDRESS<br><br>Department of Civil Engineering<br>Princeton University, Princeton, NJ    08544 | | 10. PROGRAM ELEMENT, PROJECT, TASK AREA & WORK UNIT NUMBERS<br><br>DRXRO-PR-P-15648-EL |
| 11. CONTROLLING OFFICE NAME AND ADDRESS<br>U. S. Army Research Office<br>Post Office Box 12211<br>Research Triangle Park, NC  27709 | | 12. REPORT DATE<br>April, 1983 |
| | | 13. NUMBER OF PAGES<br>48 |
| 14. MONITORING AGENCY NAME & ADDRESS(if different from Controlling Office) | | 15. SECURITY CLASS. (of this report)<br><br>Unclassified |
| | | 15a. DECLASSIFICATION/DOWNGRADING SCHEDULE |

16. DISTRIBUTION STATEMENT (of this Report)

Approved for public release; distribution unlimited.

17. DISTRIBUTION STATEMENT (of the abstract entered in Block 20, if different from Report)

18. SUPPLEMENTARY NOTES

The view, opinions, and/or findings contained in this report are those of the author(s) and should not be construed as an official Department of the Army position, policy, or decision, unless so designated by other documentation

19. KEY WORDS (Continue on reverse side if necessary and identify by block number)
Vibrations of crystal plates under initial stresses; doubly-rotated cuts Quartz Resonators; Force sensitivity, Acceleration Sensitivity; Three-point Mount, Four-point Mount.

20. ABSTRACT (Continue on reverse side if necessary and identify by block number)
- ⟩ Two-dimensional equations of motion of doubly-rotated quartz plates for the thickness-shear, flexure, and extensional vibrations under in-plane initial stresses are employed to predict changes in the fundamental thickness-shear frequencies due to initial stresses. Two types of initial stresses are considered: (1) stresses due to a pair of diametral forces, and  (2) stresses due to steady accelerations for a three-point "T" shaped mount and a four-point "+" shaped mount configurations.
    Continued on reverse. . .

DD FORM 1473  EDITION OF 1 NOV 65 IS OBSOLETE

Force sensitivity and acceleration sensitivity coefficients are computed and compared with experimental data and existing computed results. For both "T" shaped and "+" shaped mount configurations, mount orientations corresponding to the maximum and minimum of acceleration sensitivity are predicted.

## TABLE OF CONTENTS

## LIST OF FIGURES

## List of Figures - continued

# LIST OF TABLES

## ABSTRACT

Two-dimensional equations of motion of doubly-rotated quartz plates
for the thickness-shear, flexure, and extensional vibrations under in-
plane initial stresses are employed to predict changes in the fundamental
thickness-shear frequencies due to initial stresses. Two types of initial
stresses are considered: (1) stresses due to a pair of diametral forces,
and (2) stresses due to steady accelerations for a three-point "T" shaped
mount and a four-point "+" shaped mount configurations.

Force sensitivity and acceleration sensitivity coefficients are
computed and compared with experimental data and existing computed results.
For both "T" shaped and "+" shaped mount configurations, mount orientations
corresponding to the maximum and minimum of acceleration sensitivity are
predicted.

## I.  INTRODUCTION

Changes in the resonance frequencies of doubly-rotated, circular quartz plates are investigated when plates are subject to in-plane initial stresses.  Two types of initial stresses are considered:  (1) stresses due to a pair of static diametral forces, and  (2) stresses due to steady accelerations when the plate is supported by a number of ribbon supports attached to the edge of the plate.

In a previous paper, a system of six two-dimensional equations of motion of crystal plates was derived for the vibrations of the flexure, extension, face-shear, thickness-shear, thickness-twist, and thickness-stretch modes subject to initial stresses.[1]  By studying the free vibrations of these six coupled modes (without initial stresses) in a number of doubly-rotated cuts of quartz plate (yxwℓ $\theta/\phi$, with $\theta = 33.9°$, $0 < \phi < 30°$), we found that in the vicinity of the fundamental thickness-shear resonances, only thickness-shear, flexure and extensional modes are predominant.[2]  Hence, only these three modes are retained in the present study, and their governing equations are given in Section II.  In Section III, solutions of these equations are derived by the Rayleigh-Schrödinger method of perturbation. It is seen that the frequency changes, in turn, depend on the solutions of two related problems, i.e., solutions of thickness-shear, flexure, and extensional vibrations without initial stresses, and solutions of initial stress problems due to forces or accelerations.  These solutions are given, respectively, in Sections IV and V.  Finally, the changes of the fundamental thickness-shear resonances are computed in Section VI.

The present study is an extension of our previous investigations in two aspects:  (1) the stress-strain relations when referred to the plate axes

can now accommodate any doubly-rotated cut of plate, and (2) the coupled equations of motion for plate vibrations have been extended to include the extensional mode in addition to the thickness-shear and flexural modes.[1,3] We note that the solutions of initial stresses due to diametral forces and due to accelerations are unified as one by realizing that the former is a particular case of the latter as discussed in Section V.

For plates subject to diametral forces, the changes of resonance frequencies, represented by the force sensitivity coefficient $K_f$, are predicted as a function of the force orientation for various cut orientations such as AT, (yxwℓ)10°/33.9°, FC, IT, SC, and rotated X-cut. The predicted results are compared to the experimental values of Ballato,[4] Ballato and Lukaszek,[5] and calculated values of EerNisse[5] by a variational method.

For plates subject to accelerations, a three-point "T"-shaped mount and a four-point "+"-shaped mount configuration are considered. The changes of resonance frequencies, represented by the acceleration sensitivity coefficient $K_a$, for an SC-cut plate, are predicted as a function of the direction of acceleration for various mounting orientations. Also values of $|K_a|_{max}$, which is proportional to the "2g" tip over results, are computed as a function of mounting orientation $\alpha$.

It is found that for the "T"-shaped mount the minimum of acceleration sensitivity occurs at orientation angle $\alpha = -15°$ and $\alpha = 75°$, while the maximum acceleration sensitivity occurs at $\alpha = +15°$ and $\alpha = -75°$. For the "+"-shaped mount, the minimum of $|K_a|$ occurs at $\alpha = 0°$ and $\alpha = 45°$, while its maximum occurs at $\alpha = 15°$ and $\alpha = 75°$.

## II.  EQUATIONS OF MOTION FOR CRYSTAL PLATES UNDER INITIAL STRESSES

Let  $X_c$ ,  $Y_c$ , and  $Z_c$  be the crystallographic axes of α-quartz,
among which  $Z_c$  is the axis of threefold symmetry (optical axis) and  $X_c$
is one of the three axes of twofold symmetry (electrical axis).  The relations
between the crystallographic axes and the plate axes of a rotated  Y-cut
and a doubly-rotated cut of quartz plate are shown in Fig. 1, in which  X,
Y, Z or  $x_1$ ,  $x_2$ ,  $x_3$  denote the plate axes in a right-h    d coordinate
system.

A system of six equations of motion for the incrementa    otions of
the six lowest modes under static initial stresses was derived in a previous
paper.[1]  By studying the  free vibrations of these six coupled modes, i.e.,
extension, face-shear, flexure, thickness-shear, thickness-twist and
thickness-stretch, in a doubly-rotated quartz strip with a pair of traction-
free edges, we found that for a series of doubly-rotated cuts with  θ = 33.9°
but  φ = 0, 10°, 15°, 19.1°, 21.9°, 30°,  and in the vicinity of thickness-
shear cut-off frequencies, the amplitudes of the thickness-shear, flexure,
and extension are much more predominant than the other three modes.[2]
Hence by neglecting the coupling with face-shear, thickness-twist and
thickness-stretch modes in Eqs. (55) of Ref. 1, we have the two-dimensional
stress equations of motion for thickness-shear, flexure and extensional
vibrations under initial stresses:

$$\frac{\partial}{\partial x_1}\left[\left[1 + u_{1,1}^{(0)}\right]t_1^{(1)} + u_{1,3}^{(0)}t_5^{(1)}\right] + \frac{\partial}{\partial x_3}\left[\left[1 + u_{1,1}^{(0)}\right]t_5^{(1)} + u_{1,3}^{(0)}t_3^{(1)}\right]$$

$$- \left[\left[1 + u_{1,1}^{(0)}\right]t_6^{(0)} + u_{1,3}^{(0)}t_4^{(0)}\right] = \frac{2}{3}b^3\rho\ddot{u}_1^{(1)} \quad ,$$

$$\frac{\partial}{\partial x_1}\left[u_{2,1}^{(0)}t_1^{(0)} + u_{2,3}^{(0)}t_5^{(0)} + \left[1 + u_2^{(1)}\right]t_6^{(0)} + u_{2,1}^{(1)}t_1^{(1)} + u_{2,3}^{(1)}t_5^{(1)}\right.$$

$$\left. + T_1^{(0)}u_{2,1}^{(0)} + T_5^{(0)}u_{2,3}^{(0)}\right] + \frac{\partial}{\partial x_3}\left[u_{2,1}^{(0)}t_5^{(0)} + u_{2,3}^{(0)}t_3^{(0)} + \left[1 + u_2^{(1)}\right]t_4^{(0)}\right.$$

$$\left. + u_{2,1}^{(1)}t_5^{(1)} + u_{2,3}^{(1)}t_3^{(1)} + T_5^{(0)}u_{2,1}^{(0)} + T_3^{(0)}u_{2,3}^{(0)}\right] = 2b\rho\ddot{u}_2^{(0)} \quad ,$$

$$\frac{\partial}{\partial x_1}\left[\left[1 + u_{1,1}^{(0)}\right]t_1^{(0)} + u_{1,3}^{(0)}t_5^{(0)} + T_1^{(0)}u_{1,1}^{(0)} + T_5^{(0)}u_{1,3}^{(0)}\right]$$

$$+ \frac{\partial}{\partial x_3}\left[\left[1 + u_{1,1}^{(0)}\right]t_5^{(0)} + u_{1,3}^{(0)}t_3^{(0)} + T_5^{(0)}u_{1,1}^{(0)} + T_3^{(0)}u_{1,3}^{(0)}\right] = 2b\rho\ddot{u}_1^{(0)} \quad ,$$

$$(1)$$

where $T_1^{(0)}$, $T_3^{(0)}$, $T_5^{(0)}$ and $U_1^{(0)}$, $U_3^{(0)}$, $U_2^{(1)}$ are, respectively, the non-vanishing components of stress and displacement due to the in-plane initial stresses, $t_p^{(0)}$ and $t_p^{(1)}$ are the zero and first order incremental stress components, and $u_1^{(1)}$, $u_2^{(0)}$ and $u_1^{(0)}$ are the components of displacement, respectively, associated to the thickness-shear, flexure and extensional modes of incremental vibrations.

Also from Ref. 1, we have the linear stress-strain and strain-displacement relations for initial fields:

$$T_p^{(0)} = 2bC_{pq}\varepsilon_q^{(0)} \quad , \qquad (2)$$

$$E_1^{(0)} = U_{1,1}^{(0)}, \qquad E_2^{(0)} = U_2^{(1)}, \qquad E_3^{(0)} = U_{3,3}^{(0)} \ ,$$

$$2E_5^{(0)} = U_{1,3}^{(0)} = U_{3,1}^{(0)} \ . \tag{3}$$

In (2), $b$ is one-half of the thickness and $C_{pq}$ are the second order elastic stiffnesses of the plate. In obtaining the last relation in (3), we have assumed that the in-plane rotation associated with initial deformation is negligible.

The stress-strain and strain-displacement relations for the incremental vibrations are deduced, respectively, from Eqs. (50) and Eqs. (53) of Ref. 1 as follows.

$$t_p^{(0)} = 2bC_{pq}^{(0)} \kappa_{(p)} \kappa_{(q)} \eta_q^{(0)} \ ,$$

$$t_p^{(1)} = \frac{2}{3} b^3 C_{pq}^{(0)} \eta_q^{(1)} \ , \tag{4}$$

$$\eta_1^{(0)} = \left[ 1 + U_{1,1}^{(0)} \right] u_{1,1}^{(0)} + U_{2,1}^{(0)} u_{2,1}^{(0)} \ ,$$

$$\eta_4^{(0)} = U_{1,3}^{(0)} u_1^{(1)} \ ,$$

$$\eta_5^{(0)} = U_{1,3}^{(0)} u_{1,1}^{(0)} + U_{2,3}^{(0)} u_{2,1}^{(0)} \ ,$$

$$\eta_6^{(0)} = \left[ 1 + U_2^{(1)} \right] u_{2,1}^{(0)} + \left[ 1 + U_{1,1}^{(0)} \right] u_1^{(1)} \ , \tag{5}$$

$$\eta_1^{(1)} = U_{2,1}^{(1)} u_{2,1}^{(0)} + \left[ 1 + U_{1,1}^{(0)} \right] u_{1,1}^{(1)} \ ,$$

$$\eta_5^{(1)} = U_{2,3}^{(1)} u_{2,1}^{(0)} + U_{1,3}^{(0)} u_{1,1}^{(1)} \ ,$$

$$\eta_2^{(0)} = \eta_3^{(0)} = \eta_2^{(1)} = \eta_3^{(1)} = \eta_4^{(1)} = \eta_6^{(1)} = 0 \ ,$$

6

where

$$C_{pq}^{(0)} = C_{pq} + C_{pqr}E_r^{(0)} \tag{6}$$

and $C_{pqr}$ are the third-order elastic stiffnesses referred to the plate axes $(x_i)$ of the crystal plate. In (4), correction factors $\kappa_{(p)}$ have been introduced in order to improve the accuracy of the dispersion relations from the present approximate equations of motion. Their values will be given in Section IV when the free vibrations of the crystal plates without initial stresses are studied.

By considering incremental vibrational modes dependent on $x_1$ only, we may write

$$u_1^{(1)} = w(x_1)e^{i\omega t} \quad ,$$

$$u_2^{(0)} = bv(x_1)e^{i\omega t} \quad , \tag{7}$$

$$u_1^{(0)} = bu(x_1)e^{i\omega t} \quad .$$

Substitution of (7) into (5), then into (4) and (1) leads to the displacement equations of motion for steady vibration

$$\bar{T}_1 w_{,11} + \bar{T}_2 w_{,1} + \bar{T}_3 w + \bar{T}_4 v_{,11} + \bar{T}_5 v_{,1} + \bar{T}_6 u_{,11} + \bar{T}_7 u_{,1} = -\Omega^2 w \quad ,$$

$$\bar{F}_1 w_{,11} + \bar{F}_2 w_{,1} + \bar{F}_3 w + \bar{F}_4 v_{,11} + \bar{F}_5 v_{,1} + \bar{F}_6 u_{,11} + \bar{F}_7 u_{,1} = -\Omega^2 v \quad ,$$

$$\bar{E}_1 w_{,11} + \bar{E}_2 w_{,1} + \bar{E}_3 w + \bar{E}_4 v_{,11} + \bar{E}_5 v_{,1} + \bar{E}_6 u_{,11} + \bar{E}_7 u_{,1} = -\Omega^2 u \quad ,$$

$$\tag{8}$$

where $\Omega = \omega/\omega_1$ is a dimensionless frequency, $\omega_1 = (3\kappa^2 c_{66}/\rho b^2)^{1/2}$ the lowest thickness-shear cut-off frequency and $\kappa^2 = \pi^2/12$.

In (8), $\bar{T}_i$, $\bar{F}_i$, and $\bar{E}_i$ are functions dependent on the initial fields of stress and displacement and the material properties $C_{pq}$ and $C_{pqr}$. The explicit expressions of these functions are given as follows:

$$\bar{T}_1 = \frac{b^2}{3\kappa^2 C_{66}} \left\{ \left[1 + u_{1,1}^{(0)}\right]\left[c_{11}^{(0)}\left(1 + u_{1,1}^{(0)}\right) + c_{15}^{(0)} u_{1,3}^{(0)}\right] \right.$$

$$\left. + u_{1,3}^{(0)}\left[c_{51}^{(0)}\left(1 + u_{1,1}^{(0)}\right) + c_{55}^{(0)} u_{1,3}^{(0)}\right]\right\} \quad ,$$

$$\bar{T}_2 = \frac{b^2}{3\kappa^2 C_{66}} \left( \left\{\left[c_{11}^{(0)}\left(1 + u_{1,1}^{(0)}\right) + c_{15}^{(0)} u_{1,3}^{(0)}\right]\left(1 + u_{1,1}^{(0)}\right)\right\}_{,1} \right.$$

$$+ \left\{\left[c_{51}^{(0)}\left(1 + u_{1,1}^{(0)}\right) + c_{55}^{(0)} u_{1,3}^{(0)}\right]\left(1 + u_{1,1}^{(0)}\right)\right\}_{,3}$$

$$+ \left\{\left[c_{51}^{(0)}\left(1 + u_{1,1}^{(0)}\right) + c_{55}^{(0)} u_{1,3}^{(0)}\right] u_{1,3}^{(0)}\right\}_{,1}$$

$$\left. + \left\{\left[c_{31}^{(0)}\left(1 + u_{1,1}^{(0)}\right) + c_{35}^{(0)} u_{1,3}^{(0)}\right] u_{1,3}^{(0)}\right\}_{,3} \right) \quad ,$$

$$\bar{T}_3 = -\frac{1}{C_{66}} \left\{\left[c_{64}^{(0)} u_{1,3}^{(0)} + \kappa_6 c_{66}^{(0)}\left(1 + u_{1,1}^{(0)}\right)\right]\left(1 + u_{1,1}^{(0)}\right)\kappa_6 \right.$$

$$\left. + \left[c_{44}^{(0)} u_{1,3}^{(0)} + \kappa_6 c_{46}^{(0)}\left(1 + u_{1,1}^{(0)}\right)\right] u_{1,3}^{(0)}\right\} \quad ,$$

$$\bar{T}_4 = \frac{b^2}{3\kappa^2 C_{66}} \left[\left(c_{11}^{(0)} u_{2,1}^{(1)} + c_{15}^{(0)} u_{2,3}^{(1)}\right)\left(1 + u_{1,1}^{(0)}\right) \right.$$

$$\left. + \left(c_{51}^{(0)} u_{2,1}^{(1)} + c_{55}^{(0)} u_{2,3}^{(1)}\right) u_{1,3}^{(0)} \right] \quad ,$$

$$\bar{T}_5 = \frac{b^2}{3\kappa^2 c_{66}} \left\{ \left[ \left( c_{11}^{(0)} u_{2,1}^{(1)} + c_{15}^{(0)} u_{2,3}^{(1)} \right) \left( 1 + u_{1,1}^{(0)} \right) \right]_{,1} \right.$$

$$+ \left[ \left( c_{51}^{(0)} u_{2,1}^{(1)} + c_{55}^{(0)} u_{2,3}^{(1)} \right) \left( 1 + u_{1,1}^{(0)} \right) \right]_{,3}$$

$$+ \left[ \left( c_{51}^{(0)} u_{2,1}^{(1)} + c_{55}^{(0)} u_{2,3}^{(1)} \right) u_{1,3}^{(0)} \right]_{,1}$$

$$\left. + \left[ \left( c_{31}^{(0)} u_{2,1}^{(1)} + c_{35}^{(0)} u_{2,3}^{(1)} \right) u_{1,3}^{(0)} \right]_{,3} \right\}$$

$$- \frac{1}{\kappa c_{66}} \left\{ \left[ \kappa_1 c_{61}^{(0)} u_{2,1}^{(0)} + c_{65}^{(0)} u_{2,3}^{(0)} + \kappa_6 \kappa c_{66}^{(0)} \left( 1 + u_2^{(1)} \right) \right] \left( 1 + u_{1,1}^{(0)} \right) \kappa_6 \right.$$

$$\left. + \left[ \kappa_1 c_{41}^{(0)} u_{2,1}^{(0)} + c_{45}^{(0)} u_{2,3}^{(0)} + \kappa_6 \kappa c_{46}^{(0)} \left( 1 + u_2^{(1)} \right) \right] u_{1,3}^{(0)} \right\} \quad ,$$

$$\bar{T}_6 = 0 \quad ,$$

$$\bar{T}_7 = - \frac{1}{\kappa c_{66}} \left\{ \left[ \kappa_1 c_{61}^{(0)} \left( 1 + u_{1,1}^{(0)} \right) + c_{65}^{(0)} u_{1,3}^{(0)} \right] \left( 1 + u_{1,1}^{(0)} \right) \kappa_6 \right.$$

$$\left. + \left[ \kappa_1 c_{41}^{(0)} \left( 1 + u_{1,1}^{(0)} \right) + c_{45}^{(0)} u_{1,3}^{(0)} \right] u_{1,3}^{(0)} \right\} \quad ,$$

$$\bar{F}_1 = \frac{b^2}{9\kappa^2 c_{66}} \left\{ u_{2,1}^{(1)} \left[ c_{11}^{(0)} \left( 1 + u_{1,1}^{(0)} \right) + c_{15}^{(0)} u_{1,3}^{(0)} \right] + u_{2,3}^{(1)} \left[ c_{51}^{(0)} \left( 1 + u_{1,1}^{(0)} \right) \right. \right.$$

$$\left. \left. + c_{55}^{(0)} u_{2,3}^{(0)} \right] \right\} \quad .$$

$$\bar{F}_2 = \frac{b}{3\kappa c_{66}} \left\{ \left[ c_{14}^{(0)} u_{1,3}^{(0)} + c_{16}^{(0)} \left( 1 + u_{1,1}^{(0)} \right) \right] u_{2,1}^{(0)} + \left[ c_{54}^{(0)} u_{1,3}^{(0)} \right. \right.$$

$$\left. + c_{56}^{(0)} \left( 1 + u_{1,1}^{(0)} \right) \right] u_{2,3}^{(0)} + \kappa \left[ c_{64}^{(0)} u_{1,3}^{(0)} + c_{66}^{(0)} \left( 1 + u_{1,1}^{(0)} \right) \right] \left( 1 + u_2^{(1)} \right) \right\}$$

$$+ \frac{b^3}{9\kappa^2 c_{66}} \left( \left\{ u_{2,1}^{(1)} \left[ c_{11}^{(0)} \left( 1 + u_{1,1}^{(0)} \right) + c_{15}^{(0)} u_{1,3}^{(0)} \right] \right\}_{,1} \right.$$

$$+ \left\{ u_{2,1}^{(1)} \left[ c_{51}^{(0)} \left( 1 + u_{1,1}^{(0)} \right) + c_{55}^{(0)} u_{1,3}^{(0)} \right] \right\}_{,1}$$

$$+ \left\{ u_{2,1}^{(1)} \left[ c_{51}^{(0)} \left( 1 + u_{1,1}^{(0)} \right) + c_{55}^{(0)} u_{1,3}^{(0)} \right] \right\}_{,3}$$

$$\left. + \left\{ u_{2,3}^{(1)} \left[ c_{31}^{(0)} \left( 1 + u_{1,1}^{(0)} \right) + c_{35}^{(0)} u_{1,3}^{(0)} \right] \right\}_{,3} \right) \quad .$$

$$\bar{F}_4 = \frac{b}{3\kappa^2 c_{66}} \left\{ \left[ c_{11}^{(0)} u_{2,1}^{(0)} + c_{15}^{(0)} u_{2,3}^{(0)} + \kappa c_{16}^{(0)} \left( 1 + u_2^{(1)} \right) \right] u_{2,1}^{(0)} \right.$$

$$+ \left[ c_{51}^{(0)} u_{2,1}^{(0)} + c_{55}^{(0)} u_{2,3}^{(0)} + \kappa c_{56}^{(0)} \left( 1 + u_2^{(1)} \right) \right] u_{2,3}^{(0)}$$

$$+ \kappa \left[ c_{61}^{(0)} u_{2,1}^{(0)} + c_{65}^{(0)} u_{2,3}^{(0)} + \kappa c_{66}^{(0)} \left( 1 + u_2^{(1)} \right) \right] \left( 1 + u_2^{(1)} \right) + T_1^{(0)}/2b$$

$$\left. + \left( \frac{b^2}{3} \right) \left[ u_{2,1}^{(1)} \left( c_{11}^{(0)} u_{2,1}^{(1)} + c_{15}^{(0)} u_{2,3}^{(1)} \right) + u_{2,3}^{(1)} \left( c_{51}^{(0)} u_{2,1}^{(1)} + c_{55}^{(0)} u_{1,3}^{(1)} \right) \right] \right\} \quad .$$

$$\bar{F}_5 = \frac{b}{3\kappa^2 c_{66}} \Bigg( \kappa_1 \left\{ \left[ \kappa_1 c_{11}^{(0)} u_{2,1}^{(0)} + c_{15}^{(0)} u_{2,3}^{(0)} + \kappa\kappa_6 c_{16}^{(0)} \left( 1 + u_2^{(1)} \right) \right] u_{2,1}^{(0)} \right\}_{,1}$$

$$+ \left\{ \left[ \kappa_1 c_{51}^{(0)} u_{2,1}^{(0)} + c_{55}^{(0)} u_{2,3}^{(0)} + \kappa\kappa_6 c_{56}^{(0)} \left( 1 + u_2^{(1)} \right) \right] u_{2,3}^{(0)} \right\}_{,1}$$

$$+ \left\{ \left[ \kappa_1 c_{51}^{(0)} u_{2,1}^{(0)} + c_{55}^{(0)} u_{2,3}^{(0)} + \kappa\kappa_6 c_{56}^{(0)} \left( 1 + u_2^{(1)} \right) \right] u_{2,1}^{(0)} \right\}_{,3}$$

$$+ \left\{ \left[ \kappa_1 c_{31}^{(0)} u_{2,1}^{(0)} + c_{35}^{(0)} u_{2,3}^{(0)} + \kappa\kappa_6 c_{36}^{(0)} \left( 1 + u_2^{(1)} \right) \right] u_{2,3}^{(0)} \right\}_{,3}$$

$$+ \kappa \left\{ \left[ \kappa_1 c_{61}^{(0)} u_{2,1}^{(0)} + c_{65}^{(0)} u_{2,3}^{(0)} + \kappa\kappa_6 c_{66}^{(0)} \left( 1 + u_2^{(1)} \right) \right] \left( 1 + u_2^{(1)} \right) \right\}_{,1}$$

$$+ \kappa \left\{ \left[ \kappa_1 c_{41}^{(0)} u_{2,1}^{(0)} + c_{45}^{(0)} u_{2,3}^{(0)} + \kappa\kappa_6 c_{46}^{(0)} \left( 1 + u_2^{(1)} \right) \right] \left( 1 + u_2^{(1)} \right) \right\}_{,3}$$

$$+ (b^2/3) \left\{ \left[ u_{2,1}^{(1)} \left( c_{11}^{(0)} u_{2,1}^{(1)} + c_{15}^{(0)} u_{2,3}^{(1)} \right) \right]_{,1} \right.$$

$$+ \left[ u_{2,1}^{(1)} \left( c_{51}^{(0)} u_{2,1}^{(1)} + c_{55}^{(0)} u_{2,3}^{(1)} \right) \right]_{,3} + \left[ u_{2,3}^{(1)} \left( c_{51}^{(0)} u_{2,1}^{(1)} + c_{55}^{(0)} u_{2,3}^{(1)} \right) \right]_{,1}$$

$$+ \left. \left[ u_{2,3}^{(1)} \left( c_{31}^{(0)} u_{2,1}^{(1)} + c_{35}^{(0)} u_{2,3}^{(1)} \right) \right]_{,3} \right\} + (1/2b) \left( T_{1,1}^{(0)} + T_{5,3}^{(0)} \right) \Bigg) \quad ,$$

$$\bar{F}_6 = \frac{b}{3\kappa^2 c_{66}} \left\{ \left[ c_{11}^{(0)} \left( 1 + u_{1,1}^{(0)} \right) + c_{15}^{(0)} u_{1,3}^{(0)} \right] u_{2,1}^{(0)} + \left[ c_{51}^{(0)} \left( 1 + u_{1,1}^{(0)} \right) \right. \right.$$

$$\left. \left. + c_{55}^{(0)} u_{1,3}^{(0)} \right] u_{2,3}^{(0)} \right\} \quad .$$

$$\bar{F}_7 = \frac{b}{3\kappa^2 c_{66}} \left( \kappa_1 \left\{ \left[ \kappa_1 c_{11}^{(0)} \left( 1 + u_{1,1}^{(0)} \right) + c_{15}^{(0)} u_{1,3}^{(0)} \right] u_{2,1}^{(0)} \right\}_{,1} \right.$$

$$+ \left\{ \left[ \kappa_1 c_{51}^{(0)} \left( 1 + u_{1,1}^{(0)} \right) + c_{55}^{(0)} u_{1,3}^{(0)} \right] u_{2,3}^{(0)} \right\}_{,1}$$

$$+ \left\{ \left[ \kappa_1 c_{51}^{(0)} \left( 1 + u_{1,1}^{(0)} \right) + c_{55}^{(0)} u_{1,3}^{(0)} \right] u_{2,1}^{(0)} \right\}_{,3}$$

$$+ \left\{ \left[ \kappa_1 c_{31}^{(0)} \left( 1 + u_{1,1}^{(0)} \right) + c_{35}^{(0)} u_{1,3}^{(0)} \right] u_{2,3}^{(0)} \right\}_{,3}$$

$$+ \left\{ \left[ \kappa c_{61}^{(0)} \left( 1 + u_{1,1}^{(0)} \right) + c_{65}^{(0)} u_{1,3}^{(0)} \right] \left( 1 + u_2^{(1)} \right) \right\}_{,1} \kappa\kappa_6$$

$$+ \left. \left\{ \left[ \kappa_1 c_{41}^{(0)} \left( 1 + u_{1,1}^{(0)} \right) + c_{45}^{(0)} u_{1,3}^{(0)} \right] \left( 1 + u_2^{(1)} \right) \right\}_{,3} \kappa \right) \qquad ,$$

$$\bar{E}_1 = 0 \qquad ,$$

$$\bar{E}_2 = \frac{b}{3\kappa c_{66}} \left\{ \left[ c_{14}^{(0)} u_{1,3}^{(0)} + c_{16}^{(0)} \left( 1 + u_{1,1}^{(0)} \right) \right] \left( 1 + u_{1,1}^{(0)} \right) \right.$$

$$+ \left. \left[ c_{54}^{(0)} u_{1,3}^{(0)} + c_{56}^{(0)} \left( 1 + u_{1,1}^{(0)} \right) \right] u_{1,3}^{(0)} \right\} \qquad ,$$

$$\bar{E}_3 = \frac{b}{3\kappa c_{66}} \left( \kappa_1 \left\{ \left[ c_{14}^{(0)} u_{1,3}^{(0)} + \kappa_6 c_{16}^{(0)} \left( 1 + u_{1,1}^{(0)} \right) \right] \left( 1 + u_{1,1}^{(0)} \right) \right\}_{,1} \right.$$

$$+ \left\{ \left[ c_{54}^{(0)} u_{1,3}^{(0)} + \kappa_6 c_{56}^{(0)} \left( 1 + u_{1,1}^{(0)} \right) \right] \left( 1 + u_{1,1}^{(0)} \right) \right\}_{,3}$$

$$+ \left\{ \left[ c_{54}^{(0)} u_{1,3}^{(0)} + \kappa_6 c_{56}^{(0)} \left( 1 + u_{1,1}^{(0)} \right) \right] u_{1,3}^{(0)} \right\}_{,1}$$

$$+ \left. \left\{ \left[ c_{34}^{(0)} u_{1,3}^{(0)} + \kappa_6 c_{36}^{(0)} \left( 1 + u_{1,1}^{(0)} \right) \right] u_{1,3}^{(0)} \right\}_{,3} \right)$$

$$\bar{E}_4 = \frac{b}{\kappa^2 c_{66}} \left\{ \left[ c_{11}^{(0)} u_{2,1}^{(0)} + c_{15}^{(0)} u_{2,3}^{(0)} + \kappa c_{16}^{(0)} \left( 1 + u_2^{(1)} \right) \right] \left( 1 + u_{1,1}^{(0)} \right) \right.$$

$$\left. + \left[ c_{51}^{(0)} u_{2,1}^{(0)} + c_{55}^{(0)} u_{2,3}^{(0)} + \kappa c_{56}^{(0)} \left( 1 + u_2^{(1)} \right) \right] u_{1,3}^{(0)} \right\} \quad ,$$

$$\bar{E}_5 = \frac{b}{\kappa^2 c_{66}} \left( \kappa_1 \left\{ \left[ \kappa_1 c_{11}^{(0)} u_{2,1}^{(0)} + c_{15}^{(0)} u_{2,3}^{(0)} + \kappa \kappa_6 c_{16}^{(0)} \left( 1 + u_2^{(1)} \right) \right] \left( 1 + u_{1,1}^{(0)} \right) \right\}_{,1} \right.$$

$$+ \left\{ \left[ \kappa_1 c_{51}^{(0)} u_{2,1}^{(0)} + c_{55}^{(0)} u_{2,3}^{(0)} + \kappa \kappa_6 c_{56}^{(0)} \left( 1 + u_2^{(1)} \right) \right] \left( 1 + u_{1,1}^{(0)} \right) \right\}_{,3}$$

$$+ \left\{ \left[ \kappa_1 c_{51}^{(0)} u_{2,1}^{(0)} + c_{55}^{(0)} u_{2,3}^{(0)} + \kappa \kappa_6 c_{56}^{(0)} \left( 1 + u_2^{(1)} \right) \right] u_{1,3}^{(0)} \right\}_{,1}$$

$$\left. + \left\{ \left[ \kappa_1 c_{31}^{(0)} u_{2,1}^{(0)} + c_{35}^{(0)} u_{2,3}^{(0)} + \kappa \kappa_6 c_{36}^{(0)} \left( 1 + u_2^{(1)} \right) \right] u_{1,3}^{(0)} \right\}_{,3} \right) \quad ,$$

$$\bar{E}_6 = \frac{b}{3\kappa^2 c_{66}} \left\{ \left[ c_{11}^{(0)} \left( 1 + u_{1,1}^{(0)} \right) + c_{15}^{(0)} u_{1,3}^{(0)} \right] \left( 1 + u_{1,1}^{(0)} \right) \right.$$

$$\left. + \left[ c_{51}^{(0)} \left( 1 + u_{1,1}^{(0)} \right) + c_{55}^{(0)} u_{1,3}^{(0)} \right] u_{1,3}^{(0)} + T_1^{(0)}/2b \right\} \quad ,$$

$$\bar{E}_7 = \frac{b^2}{3\kappa^2 c_{66}} \left( \kappa_1 \left\{ \left[ \kappa_1 c_{11}^{(0)} \left( 1 + u_{1,1}^{(0)} \right) + c_{15}^{(0)} u_{1,3}^{(0)} \right] \left( 1 + u_{1,1}^{(0)} \right) \right\}_{,1} \right.$$

$$+ \left\{ \left[ \kappa_1 c_{51}^{(0)} \left( 1 + u_{1,1}^{(0)} \right) + c_{55}^{(0)} u_{1,3}^{(0)} \right] \left( 1 + u_{1,1}^{(0)} \right) \right\}_{,3}$$

$$+ \left\{ \left[ \kappa_1 c_{51}^{(0)} \left( 1 + u_{1,1}^{(0)} \right) + c_{55}^{(0)} u_{1,3}^{(0)} \right] u_{1,3}^{(0)} \right\}_{,1}$$

$$\left. + \left\{ \left[ \kappa_1 c_{31}^{(0)} \left( 1 + u_{1,1}^{(0)} \right) + c_{35}^{(0)} u_{1,3}^{(0)} \right] u_{1,3}^{(0)} \right\}_{,3} + \left( \frac{1}{2b} \right) \left( T_{1,1}^{(0)} + T_{5,3}^{(0)} \right) \right) \quad .$$

(9)

Once the initial fields of stress and displacement are determined from the solutions of initial stress problems which will be discussed in Section V, then these functions of (9) may be regarded as known functions of $x_1$ and $x_3$. Each of these functions may be separated into two parts as

$$\bar{T}_i = T_i + t_i, \quad \bar{F}_i = F_i + f_i, \quad \bar{E}_i = E_i + e_i, \tag{10}$$

where $T_i$, $F_i$ and $E_i$ are associated with vibrational motions without initial stresses, while $t_i$, $f_i$, and $e_i$ are the quantities contributed by the initial fields.[3] Therefore, by setting initial stresses and displacement gradients in (9) equal to zero, we obtain

$$T_1 = \frac{b^2 C_{11}}{3\kappa^2 C_{66}}, \quad T_3 = T_5 = -\kappa_6^2, \quad T_7 = \frac{\kappa_1 \kappa_6 C_{16}}{\kappa C_{66}},$$

$$F_2 = F_4 = \frac{b}{3}, \quad F_6 = E_2 = E_4 = \frac{b C_{16}}{3\kappa C_{66}}, \quad E_6 = \frac{b C_{11}}{3\kappa^2 C_{66}},$$

$$T_2 = T_4 = T_6 = F_1 = F_3 = F_5 = F_7 = E_1 = E_3 = E_5 = E_7 = 0 \quad . \tag{11}$$

The explicit expressions for $t_i$, $f_i$ and $e_i$ are obtained by inserting (9) and (11) into (10).

## III. SOLUTIONS BY PERTURBATION METHOD

For the thickness-shear, flexure, and extensional vibrations under static initial stresses, (8) can be expressed in the matrix form

$$LV = \lambda V \tag{12}$$

where $\lambda = -\Omega^2$ is the eigenvalue, $V = (w,v,u)^T$ the displacement vector, and $L$ the linear differential operator. By inserting (10) into (8), we may separate $L$ into two parts

$$L = L_0 + Q \tag{13}$$

where

$$L_0 = \begin{bmatrix} T_1\partial_{11} + T_3 & T_5\partial_1 & T_7\partial_1 \\ F_2\partial_1 & F_4\partial_{11} & F_6\partial_{11} \\ E_2\partial_1 & E_4\partial_{11} & E_6\partial_{11} \end{bmatrix} , \tag{14}$$

$$Q = \begin{bmatrix} t_1\partial_{11}+t_2\partial_1+t_3 & t_4\partial_{11}+t_5\partial_1 & t_7\partial_1 \\ f_1\partial_{11}+f_2\partial_1+f_3 & f_4\partial_{11}+f_5\partial_1 & f_6\partial_{11}+f_7\partial_1 \\ e_2\partial_1 + e_3 & e_4\partial_{11}+e_5\partial_1 & e_6\partial_{11}+e_7\partial_1 \end{bmatrix} . \tag{15}$$

$L_0$ is the part of the operator associated with vibrations without initial stresses, while $Q$ is the part of the operator containing all the effects of the initial stresses inside the plate. In general, initial stresses also affects the traction boundary conditions, for instance, as shown in Eqs. (52) of Ref. 1. However, we will neglect contributions of initial stresses to the traction boundary conditions by assuming that these effects at the edge of the plate have little influence on the

fundamental thickness-shear vibration whose displacement is mostly confined in the central portion of the plate. For instance, by neglecting the initial fields in (4), the traction-free conditions

$$t_1^{(1)} = t_6^{(0)} = t_1^{(0)} = 0 \qquad \text{at} \quad x_1 = \pm a \tag{16}$$

may be expressed by

$$PV = 0 \qquad \text{at} \quad x_1 = \pm a , \tag{17}$$

where the linear operation $P$ is given by

$$P = \begin{bmatrix} c_{11}\partial_1 & 0 & 0 \\ \kappa\kappa_6 c_{66} & \kappa\kappa_6 c_{66}\partial_1 & \kappa\kappa_1 c_{16}\partial_1 \\ \kappa\kappa_6 c_{16} & \kappa\kappa_6 c_{16}\partial_1 & \kappa\kappa_1 c_{11}\partial_1 \end{bmatrix} . \tag{18}$$

From previous calculations of the initial stress fields,[1,3] we found that the values of $t_i$, $f_i$, and $e_i$ are of several orders of magnitude smaller than those of $T_i$, $F_i$, and $E_i$, respectively. Hence, we employ the Rayleigh-Schrödinger method of perturbation to calculate the frequency changes due to initial stresses.

Let $V_n$ and $\lambda_n$ be the eigenvector and eigenvalue, respectively, of the $n^{th}$ mode satisfying (12) and (17). Therefore,

$$LV_n = \lambda_n V_n, \qquad PV_n = 0 \quad \text{at} \quad x_1 = \pm a \tag{19}$$

where

$$L = L_0 + \varepsilon Q_1 , \quad Q = \varepsilon Q_1 . \tag{20}$$

A small parameter $\varepsilon$ is introduced in (20) to indicate the smallness of $Q$ as compared to $L_0$, while $Q_1$ is assumed to have the same order of magnitude as $L_0$. We let

$$V_n = V_{n0} + \epsilon V_{n1} + \ldots \quad ,$$

$$\lambda_n = \lambda_{n0} + \epsilon \lambda_{n1} + \ldots \quad . \tag{21}$$

Substitution of (21) into (19) and collection of the zero and first order terms of $\epsilon$ leads to

$$L_0 V_{n0} = \lambda_{n0} V_{n0}, \qquad P V_{n0} = 0 \qquad \text{at } x_1 = \pm a \tag{22}$$

$$L_0 V_{n1} + Q_1 V_{n0} = \lambda_{n0} V_{n1} + \lambda_{n1} V_{n0}, \quad P V_{n1} = 0 \qquad \text{at } x_1 = \pm a \ . \tag{23}$$

We see that (22) corresponds to plate vibrations without initial stresses and with traction-free edge conditions. $L_0$ is a symmetric operator and $V_{n0}$'s are free-vibrational modes forming a complete, othonormal set (after normalization). Therefore

$$V_{m0} \cdot V_{n0} = \delta_{mn} \tag{24}$$

In (23), $\lambda_{n1}$ and $V_{n1}$ are the first order perturbations of $\lambda_n$ and $V_n$, respectively. We let

$$V_{n1} = \sum_m a_{nm} V_{n0} \quad . \tag{25}$$

By inserting (25) into the first equation of (23), multiplying the resulting equation by $V_{n0}$ and employing (24), we obtain

$$\lambda_{n1} = V_{n0} \cdot Q_1 \cdot V_{n0}$$

$$\text{or} \quad \epsilon \lambda_{n1} = V_{n0} \cdot \epsilon Q_1 \cdot V_{n0} = V_{n0} \cdot Q \cdot V_{n0} \tag{26}$$

The second equation of (23) is also satisfied by (25) because $V_{n0}$ satisfy the second of (22).

We choose $n=1$ to indicate the fundamental thickness-shear mode of vibration. From the second of (21), we have

$$\lambda_1 = \lambda_{10} + \epsilon\lambda_{11} \qquad \text{or} \qquad \Omega_1^2 = \Omega_{10}^2 + \epsilon\Omega_{11}^2 \qquad\qquad (27)$$

where $\Omega_{10}$ is the resonance frequency of the fundamental thickness-shear without initial stresses. The frequency changes, by (27) and (26), can be expressed by

$$\frac{\Delta f}{f_0} = \frac{\Omega_1 - \Omega_{10}}{\Omega_{10}} = \frac{\Omega_1^2 - \Omega_{10}^2}{2\Omega_{10}^2} = \frac{\epsilon\lambda_{11}}{2\lambda_{10}} = \frac{V_{10} \cdot Q \cdot V_{10}}{2\lambda_{10}} \qquad . \qquad (28)$$

To compute the changes of frequencies from (28), we need $V_{10}$ and $\lambda_{10}$ from the solutions of free vibrations of crystal plates (see Section IV) and $Q$ from the solutions of initial stress problems (see Section V).

## IV.   THICKNESS-SHEAR, FLEXURAL AND EXTENSIONAL VIBRATIONS

## OF DOUBLY-ROTATED QUARTZ PLATES

For the resonance frequencies $(\lambda_{10} = -\Omega_{10}^2)$ and the vibrational modes $V_{10} = (w, v, u)^T$, we should look for solutions satisfying the two-dimensional governing plate equations and traction-free conditions at the edge of a circular crystal plate.   An analytical solution for such a problem is extremely complex and difficult to obtain, if not impossible. However at predominantly fundamental thickness-shear resonances, the vibrational motion is mostly confined in the middle portion of a flat plate.   This mode is concentrated even more in the central portion of a contoured or electrode plated plate.[6,7]   Furthermore, the thickness-shear resonance frequencies are shown to be insensitive to the width of a rectangular plate by Sykes[8] and predictions from one-dimensional solutions are shown to be very accurate when they are compared with experimental data.[9,10]   Therefore in this section of the paper, the circular plate is approximated by a square plate of equivalent area and one-dimensional solutions are obtained to predict resonance frequencies and vibrational modes.

The one-dimensional equations of motion and traction-free edge conditions at $x_1 = \pm a$ ($2a = \sqrt{\pi}\, R$, $R$ = radius of the circular plate) are given by (22), with $L_0$ and $P$ defined, respecitvely, by (14) and (18), and $n = 1$.

We assume that displacement $V_{10} = (w,v,u)^T$ has the vibrational form

$$w = \sum_{q=1}^{3} A_{1q} \cos \xi_q x_1 \quad ,$$

$$v = \sum_{q=1}^{3} A_{2q} \sin \xi_q x_1 \quad ,$$

$$u = \sum_{q=1}^{3} A_{3q} \sin \xi_q x_1 \quad . \tag{29}$$

By substituting (29) into the first of (22), we have the dispersion relation ($\Omega$ vs. $\xi_q$, $q=1,2,3$)

$$\begin{vmatrix} 3\Omega^2 - \bar{\xi}_q^2 \bar{c}_{11} & -\bar{\xi}_q^2 \bar{c}_{16} & -\bar{\xi}_q \bar{c}_{16} \\ -\bar{\xi}_q^2 \bar{c}_{16} & 3\Omega^2 - \bar{\xi}_q^2 \bar{c}_{66} & -\bar{\xi}_q \bar{c}_{66} \\ -\bar{\xi}_q \bar{c}_{16} & -\bar{\xi}_q \bar{c}_{66} & \Omega^2 - \bar{c}_{66} - \dfrac{\bar{\xi}_q^2 \bar{c}_{11}}{3\kappa_1^2} \end{vmatrix} = 0 \tag{30}$$

where $\bar{\xi}_q = \xi_q b$ are the dimensionless wave numbers and the roots of the above bicubic equation in $\Omega$ and $\bar{\xi}$ for a given value of $\Omega$, and

$$\bar{c}_{pq} = \kappa_{(p)} \kappa_{(q)} c_{pq} / \kappa^2 c_{66} \quad . \tag{31}$$

From the linear, homogeneous equations governing the displacement amplitudes, we obtain the amplitude ratios

$$A_{1q} : A_{2q} : A_{3q} = 1 : \alpha_{2q} : \alpha_{3q} \quad , \qquad q=1,2,3 \tag{32}$$

where

$$\alpha_{2q} = D^{-1} \begin{vmatrix} \bar{\xi}_q \bar{c}_{16} & -\bar{\xi}_q^2 \bar{c}_{16} \\ \bar{\xi}_q \bar{c}_{66} & 3\Omega^2 - \bar{\xi}_q^2 \bar{c}_{66} \end{vmatrix} \quad ,$$

$$\alpha_{3q} = D^{-1} \begin{vmatrix} 3\Omega^2 - \bar{\xi}_q^2 \bar{c}_{11} & \bar{\xi}_q \bar{c}_{16} \\ -\bar{\xi}_q^2 \bar{c}_{16} & \bar{\xi}_q \bar{c}_{66} \end{vmatrix} \quad ,$$

$$D = \begin{vmatrix} 3\Omega^2 - \bar{\xi}_q^2 \bar{c}_{11} & -\bar{\xi}_q^2 \bar{c}_{16} \\ -\bar{\xi}_q^2 \bar{c}_{16} & 3\Omega^2 - \bar{\xi}_q^2 \bar{c}_{66} \end{vmatrix} . \qquad (33)$$

Correction factors $\kappa_{(p)}$ introduced in (4) and consequently appeared in (9), (11), (30) and (31) are given below

$$\kappa_{(p)} = \begin{cases} 1 & \text{if } p = 3,5 \\ \kappa = \dfrac{\pi}{\sqrt{12}} & \text{if } p = 2,4 \\ \kappa_1 & \text{if } p = 1 \\ \kappa\kappa_6 = \dfrac{\pi}{\sqrt{12}}\Omega_c & \text{if } p = 6 \end{cases} \qquad (34)$$

In a previous study[2] of free vibrations of the first six modes in doubly-rotated quartz plates, correction factors are introduced to correct the cut-off frequencies of thickness-stretch, thickness-twist, and thickness-shear modes (or called a, b, and c modes, respectively) by letting

$$\kappa_{(p)} = \begin{cases} 1 & \text{if } p = 1,3,5 \\ \kappa = \dfrac{\pi}{\sqrt{12}} & \text{if } p = 2,4,6. \end{cases}$$

Since only three of the six modes are included in the present study, two new correction factors $\kappa_1$ and $\kappa_6$ are introduced in (34) to correct the behavior of the dispersion relation from the three-mode theory as compared to that of the six-mode theory. $\kappa_6$ is employed for correcting the thickness-shear cut-off frequencies and $\kappa_1$ for adjusting the slope of the extensional branch ($E_1$). The values of $\kappa_1$ and $\kappa_6$ for various cuts of quartz plate are listed in Table 1.

Dispersion curves computed from (30) for an SC-cut quartz plate are shown in Fig. 2 by the solid lines as compared with those in dashed lines computed from the six coupled equations of motion.[2] It may be seen that the three corresponding frequency branches from the three-mode and six-mode theories agree closely for frequencies up to and including the fundamental thickness-shear cut-off frequency.

Substitution of (29) into the second of (22) for traction-free edge conditions leads to three linear homogeneous equations on $A_{1q}$

$$[M_{pq}]\{A_{1q}\} = 0, \qquad p,q = 1,2,3 \tag{35}$$

where

$$M_{1q} = C_{11}\xi_q \sin \xi_q a \quad ,$$

$$M_{2q} = [\kappa_1 C_{61}\alpha_{3q}\xi_q + \kappa\kappa_6 C_{66}(1 + \alpha_{2q}\xi_q)]\cos \xi_q a \quad ,$$

$$M_{3q} = [\kappa_1 C_{11}\alpha_{3q}\xi_q + \kappa\kappa_6 C_{16}(1 + \alpha_{2q}\xi_q)]\cos \xi_q a \quad . \tag{36}$$

For nontrivial solutions of (35), we have

$$\det M_{pq} = 0 \tag{37}$$

which is the frequency equation for the thickness-shear, flexural, and extensional vibrations.

Calculations of the resonance frequencies of SC-cut plates are performed and illustrated in Fig. 3. By comparing Fig. 3 with Figs. 4 and 5, which are the corresponding frequency spectra calculated from the six-mode theory,[2] we see that the present three-mode theory gives very good predictions for frequencies of thickness-shear, flexural, and extensional modes.

From (35), we can also calculate the amplitude ratios

$$A_{11} : A_{12} : A_{13} = 1 : \beta_2 : \beta_3 \qquad (38)$$

if we choose $A_{11}$ as the reference. Then the displacement field (29) can be expressed in terms of $\alpha_{pq}$ and $\beta_q$ (with $\beta_1 = 1$)

$$V_{10} = \left\{ \begin{array}{c} w \\ v \\ u \end{array} \right\} = A_{11} \left\{ \begin{array}{c} \sum\limits_{q=1}^{3} \beta_q \cos \xi_q x_1 \\[2ex] \sum\limits_{q=1}^{3} \beta_q \alpha_{2q} \sin \xi_q x_1 \\[2ex] \sum\limits_{q=1}^{3} \beta_q \alpha_{3q} \sin \xi_q x_1 \end{array} \right\} \qquad (39)$$

The remaining constant $A_{11}$ can be determined from the normalization condition (24), i.e.,

$$V_{10} \cdot V_{10} = \int_A \{w\ v\ u\} \left\{ \begin{array}{c} w \\ v \\ u \end{array} \right\} dA = 1 \qquad . \qquad (40)$$

## V.  INITIAL STRESSES IN CIRCULAR PLATES

Two types of initial stress problems are considered in this section.

### 1.  Circular plates subject to a pair of diametral forces.

A circular plate of diameter $d(= 2R)$ and thickness $2b$ is referred to a rectangular coordinate system $X, Y, Z$ (or $x_i$) with the $XZ$ plane being the middle plane of the plate.  Let $N$ be the magnitude of the compressive diametral forces and $\psi$ (the azimuth angle) to denote the orientation of the force with respect to the $X$ axis as shown in Fig. 6.

### 2.  Circular plates subject to in-plane, steady acceleration.

The same plate is now supported by a number of metal ribbons attached to the edge of the plate as shown in Fig. 7.  The locations of the supports are denoted by angles $\alpha_i$, $i = 1,2,3\ldots s$ for $s$ supports $(s \geq 2)$.  The orientation of the body force $\underset{\sim}{G}$ (force per unit volume) which has the opposite sense to the acceleration is denoted by the angle $\psi$ with respect to the $X$ axis as shown in both Figs. 1 and 7.  Let $N_i$ and $T_i$ be, respectively, the normal and tangential components of the force from the support at $\alpha_i$ to the plate.

Effects of initial stresses of both types on the changes in the thickness-shear resonance frequencies had been studied previously for rotated Y-cuts of quartz plate.[1,3]  In both cases the initial stresses were obtained from solutions for isotropic plates, then strains were calculated from the anisotropic stress-strain relations.  The predicted results were compared with experimental data with good agreement for AT- and Y-cuts.

In the present paper, the same approach is adopted.  Since the initial stresses due to acceleration, problem (2), have been given in detail in Ref. 3, Eqs. (1) - (11), they will not be duplicated here.

We would like to note that the solution for the problem (1), initial stresses due to the diametral forces, can be deduced from that of the problem (2) by setting

$$s = 2, \qquad \underset{\sim}{G} = 0,$$

$$\alpha_1 = \psi, \qquad \alpha_2 = \alpha_1 + 180°,$$

$$N_1 = N_2 = -N,$$

$$T_1 = T_2 = 0, \tag{41}$$

in Eqs. (1) - (11) of Ref. 3.

In a study by Janiand, Nissim, and Gagnepain,[11] initial stresses were obtained directly for the anisotropic plates and employed to predict the changes in frequencies. It showed some improvement in predictions of frequency changes due to diametral forces, but almost no improvement for the case of acceleration effect.

## VI. CHANGES IN RESONANCE FREQUENCIES

Once the resonance frequencies $\lambda_{10}(= -\Omega_{10}^2)$ is obtained from (37), displacement field $V_{10}$ from (39), and $Q$ from (15) and initial fields given in Section V, the frequency changes due to initial stresses can be obtained by numerical integration of (28)

$$\frac{\Delta f}{f_0} = \frac{1}{2\lambda_{10}} \int_A V_{10} \cdot Q \cdot V_{10} dA \qquad (28)'$$

where $A$ is the electroded area of the plate.

### (1) Effect due to a pair of Diametral Forces

Following Ratajski's[12] definition of force sensitivity coefficient, we have

$$K_f = \frac{\Delta f}{f_0} \cdot \frac{1}{N} \cdot \frac{d}{f_0/m} = \frac{\Delta f}{f_0} \frac{bd}{N} \sqrt{\frac{\rho}{C_{66}}} = F(\theta,\phi;\psi) \qquad (42)$$

where $N$ is the magnitude of diametral forces, $m$ the order of harmonic overtones of the thickness-shear frequencies, and $\theta,\phi$ are the angles of rotation for doubly-rotated cut as shown in Fig. 1.

Computations of $K_f$ as a function of the orientation of the diametral forces $\psi$ are made for circular quartz plates of AT-cut $(yx\ell)33.9°$, $(yxw\ell)10°/33.9°$, FC-cut $(yxw\ell)15°/33.9°$, IT-cut $(yxw\ell)19°/33.9°$, SC-cut $(yxw\ell)22°/33.9°$, and rotated X-cut $(yxw\ell)30°/33.9°$. The results are shown in Figs. 8 to 13, respectively. They are compared with the experimental results of Ballato,[4] Ballato and Lukaszek,[5] and the calculated result of EerNisse.[5] The results of Refs. 5 and 11 both show the improvement of predicted frequencies by employing the initial stress field of anisotropic plates under a pair of diametral forces.

## (2)  Effect due to Steady Accelerations

We define the acceleration sensitivity coefficient

$$K_a = \frac{\Delta f}{f_0} \cdot \frac{1}{B} \cdot \frac{d}{f_0 \sqrt{m}} = \frac{\Delta f}{f_0} \frac{8/\pi}{ngd\sqrt{\rho C_{66}}} = F(\theta,\phi;\alpha_i;\psi) \tag{43}$$

where  $B = ng\rho(\pi bd^2/2)$  is the magnitude of body force on the plate and

ng  the acceleration in terms of the acceleration of gravity.

As indicated in (43),  $K_a$  is also dependent on the positions of

supports of the plate.  Two support configurations are considered as

follows.

### (a)  Three-point "T" shaped mount

A support configuration of a circular plate with three supports

of which two supports are 180° apart and the third is 90° from the

first two forming a "T" shape is called a "T" shaped mount as shown in

Fig. 14.  The angle  $\alpha$  denotes the orientation of the "T" shaped mount,

while  $\psi$  indicates the orientation of the body force due to acceleration.

Calculations are made for a circular SC-cut plate (yxwℓ)23.75°/33.9°.

$K_a$  is computed as a function of  $\psi$  for  $\alpha = 0°,-15°,-30°$, and $-45°$,

and is plotted in Fig. 14.  We see that both the magnitude and location

of  $|K_a|_{max}$  change as the support orientation  $\alpha$  changes.  By repeating

the above process of calculation, we obtain  $|K_a|_{max}$  as a function of

$\alpha$  as given in Fig. 15.  It can be seen from Fig. 15 that the minimum

acceleration-sensitivity occurs at  $\alpha = -15°$ and $+75°$, while the maximum

acceleration-sensitivity occurs at  $\alpha = +15°$ and  $\alpha = -75°$.  The variation

of acceleration sensitivity as a function of  $\alpha$  for  "T" shaped mount

has been studied experimentally by Goldfrank and Warner and their experi-

mental values are shown as solid dots in Fig. 15 for comparison.[13]

The result shown in Fig. 15 is also consistent qualitatively with the experimental data by Kusters, Adams and Yoshida,[14] for their study is on a two-point mount configuration (see Fig. 2 of Ref. 14). We note the convention for the mounting angles in Ref. 14 is the opposite of that employed in the present paper.

### (b) Four-point "+" Shaped Mount

A four-point support configuration of a circular plate for which each support is 90° from its neighboring supports is called a four-point "+" shaped mount. Computations on an SC-cut circular plate have been carried out in similar manner as in case (a). The plots of $K_a$ vs. $\psi$ for various values of $\alpha$ and $|K_a|_{max}$ vs. $\alpha$ are given in Figs. 16 and 17, respectively.

Figure 17 reveals that the minimum of acceleration sensitivity occurs at $\alpha = 0°$ (or 90°) and $\alpha = 45°$ (or -45°), while the maximum occurs at $\alpha = 15°$ and $\alpha = 75°$. It may be seen that there exists a wider "valley" at $\alpha = 45°$ than that at $\alpha = 0°$. It therefore appears to suggest that it is more likely to obtain experimentally a $|K_a| =$ minimum near $\alpha = 45°$ than at $\alpha = 0°$. Nevertheless, a minimum of $|K_a|$ at $\alpha = 0°$ had been attained experimentally by Warner.[15]

The effect of small deviations of the support locations from the 90° angle in the "+" shaped mount has also been investigated by allowing one or two supports having an angle of deviation $\delta$ for $-3° \leq \delta \leq 3°$. Results from several series of computations shows that the magnitude of acceleration coefficient $|K_a|$ increases as $|\delta|$ increases for small deviations $-3° \leq \delta \leq 3°$. However, the $|K_a|_{max}$ vs. $\alpha$ relation remains practically the same as that shown in Fig. 17, therefore it is independent of $\delta$.

In all the calculations, we have employed Bechmann's values of the second-order elastic stiffnesses[16] and those of Thurston, McSkimin and Andreath for the third-order elastic stiffnesses[17] of quartz. For calculating support reactions from ribbon supports due to accelerations, we have assumed each ribbon support is made of nickel and acts as a cantilever with length $\ell = 6.35$ mm and rectangular cross section ($h_1 = 0.076$ mm and $h_2 = 1.270$ mm). The Young's modulus for nickel is $E = 4.82 \times 10^9$ dyn/cm$^2$. For more detail, see Eq. (2) of Ref. 3.

## ACKNOWLEDGMENT

## REFERENCES

1. Lee, P. C. Y., Wang, Y. S. and Markenscoff, X., Proc. 27th Ann. Freq. Cont. Symp. 1-6 (1973), also J. Acoust. Soc. Am., Vol. 57, 95 (1975).

2. Lee, P. C. Y. and Wu, Kuang-Ming, presented at the 33rd Freq. Control Symposium (1979).

3. Lee, P. C. Y. and Wu, K-M, Proc. 30th Ann. Freq. Contr. Symp. 1-7, (1976), also J.Acoust. Soc. Am., Vol. 63, 1039-1047 (1977).

4. Ballato, A. D., Proc. 14th Ann. Freq. Cont. Symp., 89-114 (1960).

5. Ballato,A.,EerNisse, E. P. and Lukaszek, T., Proc. 31st Ann. Freq. Cont. Symp., 8-10, (1977).

6. Lee. P. C. Y. and Chen, S.S., J. Acoust. Soc. Amer., 46, 1193-1202 (1969).

7. Lee, P. C. Y., and Spencer, W. J., J. Acoust. Soc. Amer., Vol. 45, 637-645, (1969).

8. Sykes, R. A., "Quartz Crystals for Electric Circuits," R. A. Heising, Editor, D. Van Nostrand, New York (1946).

9. Mindlin, R. D. and Gazis, D. C., Proc. 4th U.S. Natl. Congr. App. Mech., 305-310 (1962).

10. Mindlin, R. D. and Lee, P. C. Y., Int. J. Solids Structures, Vol. 2, 125-139 (1966).

11. Janiand, D., Nissim, L. and Gagnepain, J. J., Proc. 32nd Ann. Freq. Cont. Symp. 169-179, (1978).

12. Ratajski, J. M., IBM No. 60-825-1940A, IBM Federal System Div., Electronics Center (1966).

13. Goldfrank, B., and Warner, A., Research and Development Technical Report DELET-TR-79-0272-3, U.S. Army Electronics Research and Development Command, Fort Monmouth, NJ, June (1981).

14. Kusters, J. A., Adams, C. A. and Yoshida, H., Proc. 31st Ann. Freq. Cont. Symp. 3-7, (1977).

15. Warner, A. 11th Interim Report, Report No. 27480-J, Bell Telephone Labs., July (1959).

16. Bechmann, R., Phys. Rev., Vol. 100, 1060-1061 (1958).

17. Thurston, R. N., McSkimin, H. J., and Andreath, P. Jr., J. Appl. Phys. Vol. 37, 267-275 (1966).

Table 1

Values of correction factors $\kappa_1$ and $\kappa_6$

for doubly-rotated quartz plates

| Doubly rotated quartz plates (yxwℓ) φ/θ, θ=33.9° | $\kappa_1$ | $\kappa_6$ |
|---|---|---|
| AT-cut, φ = 0° | 1.0 | 1.0 |
| φ = 10° | 1.0116 | 0.9818 |
| FC-cut, φ = 15° | 1.0214 | 0.963 |
| IT-cut, φ = 19.1° | 1.0252 | 0.9492 |
| SC-cut, φ = 21.9° | 1.0252 | 0.9397 |
| Rotated-X-cut, φ = 30° | 1.0146 | 0.918 |
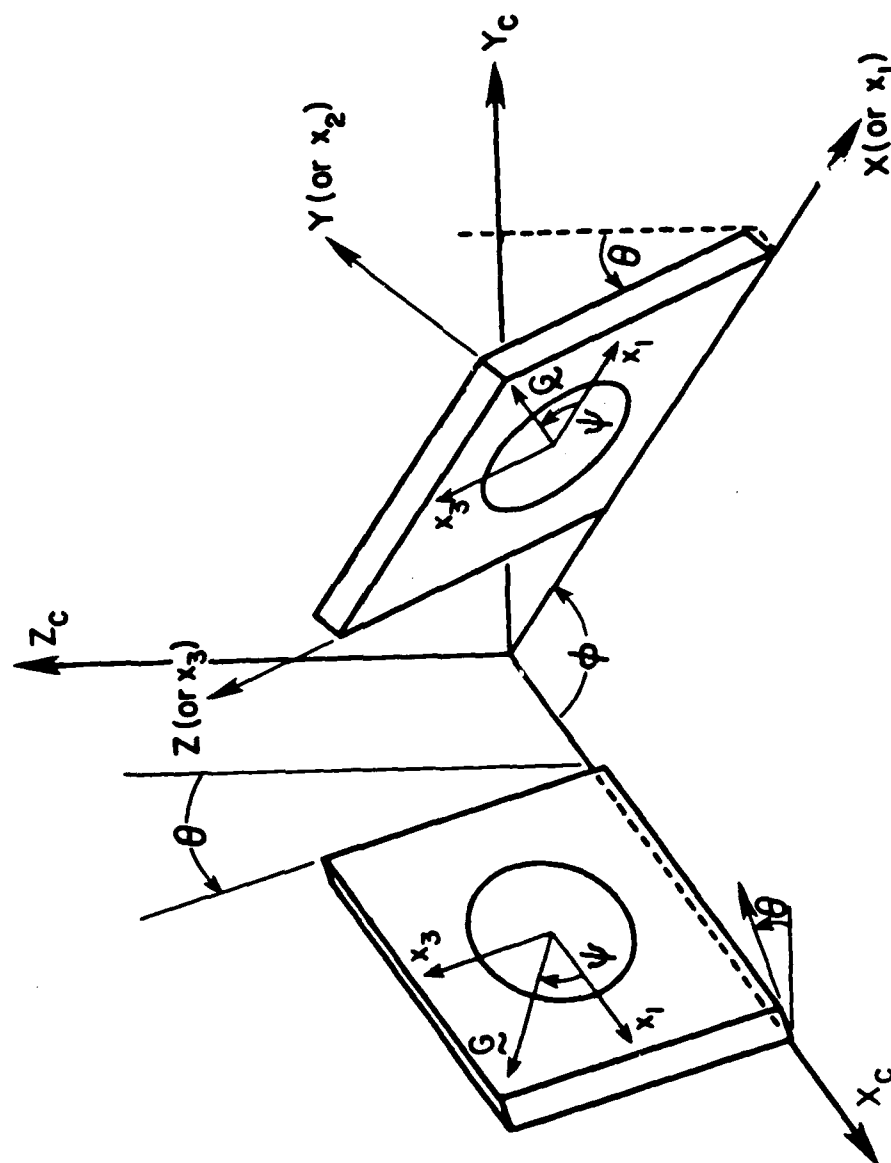
Fig. 1  Plate orientations $(x_i)$ with respect to crystal axes $X_c$, $Y_c$, $Z_c$ for singly and doubly rotated plates.

33
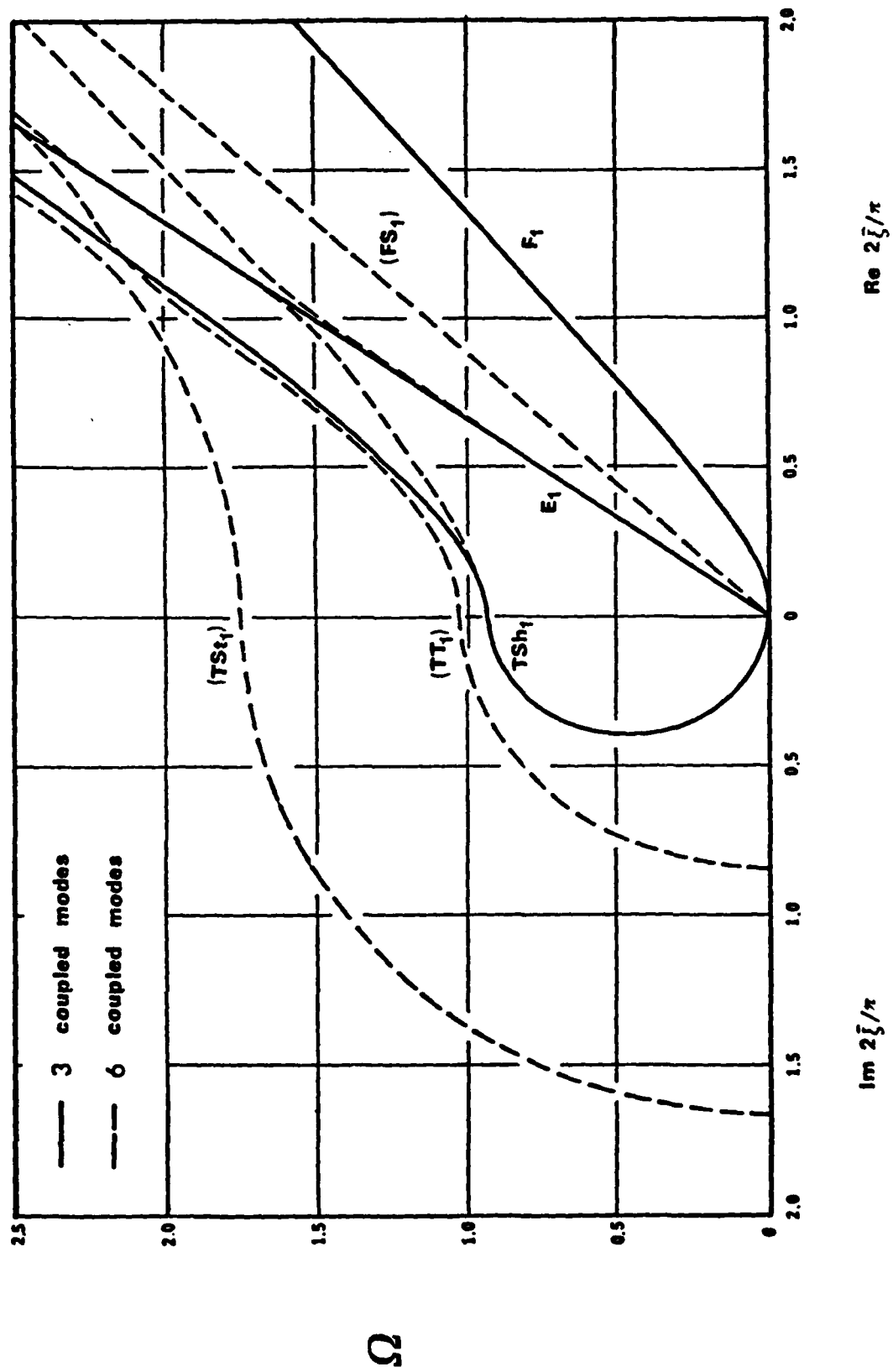


Fig. 2  Dispersion curves of SC-cut quartz plate for waves propagating in the $x_1$-direction.

34
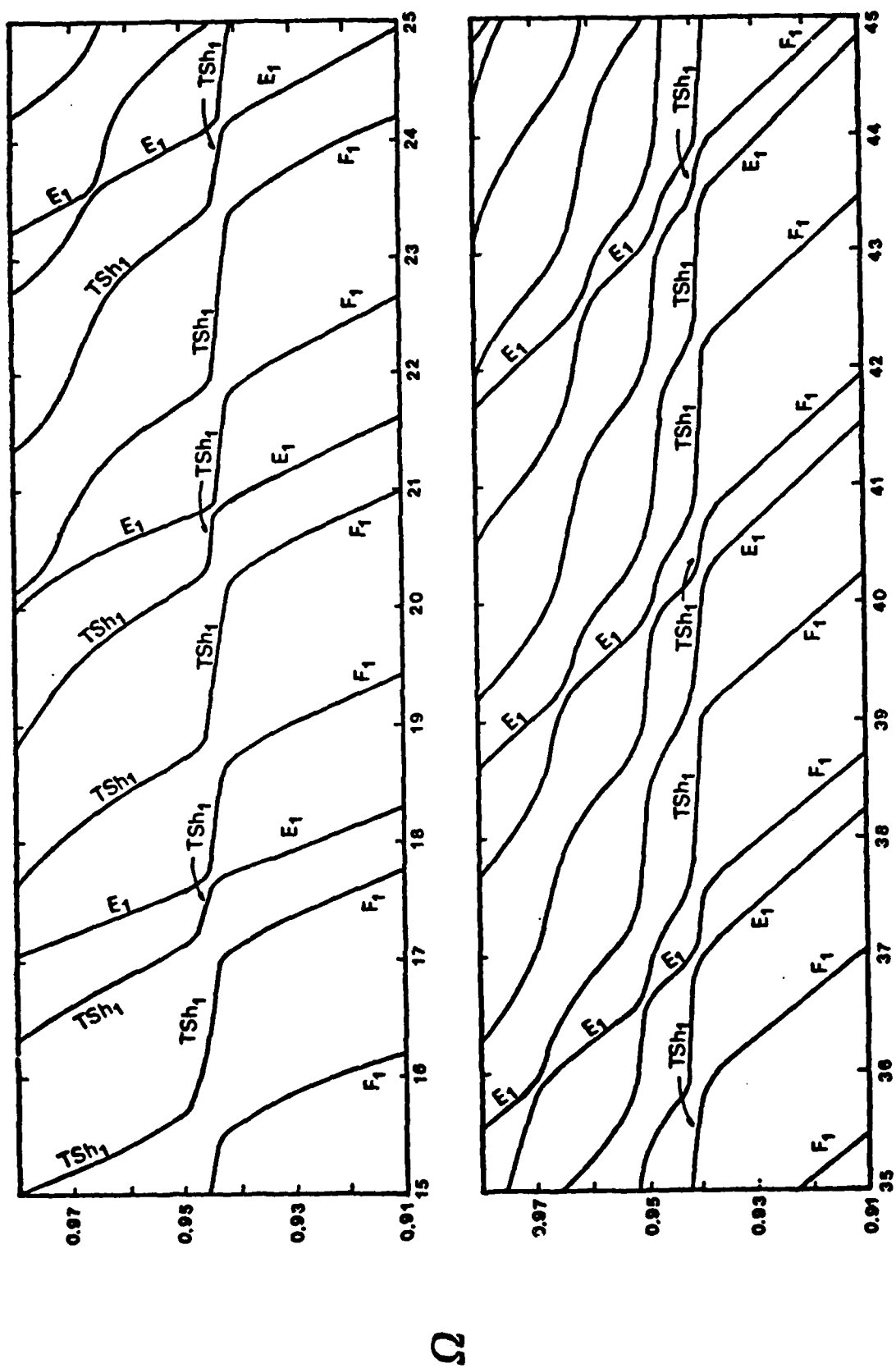


Fig. 3 Frequency spectra of SC-cut quartz plate for waves propagating in the $x_1$-direction.
(3 modes)
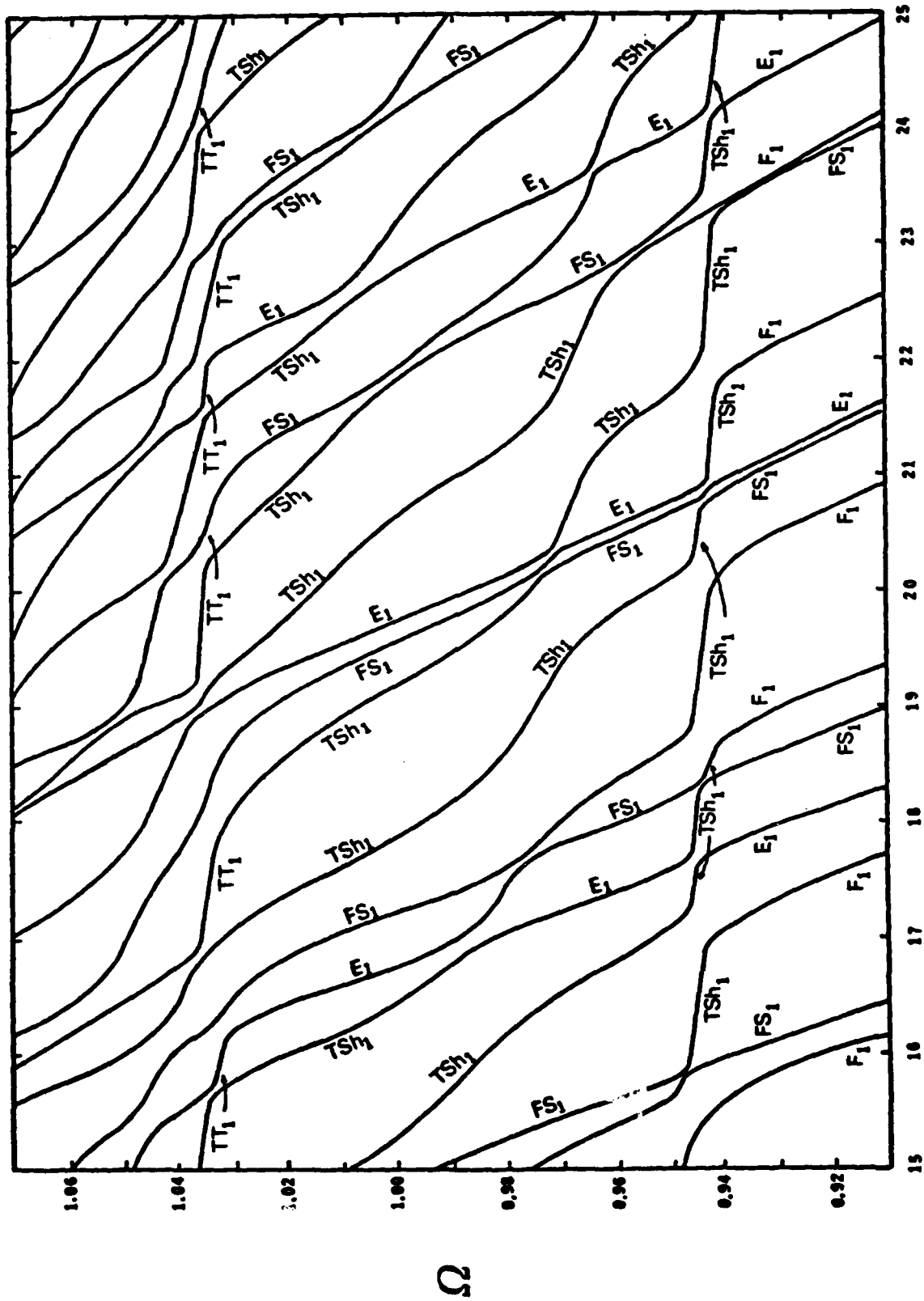
Fig. 4 Frequency spectra of SC-cut quartz plate for waves propagating in the $x_1$-direction ($15 \leq a/b \leq 25$). (6 modes)
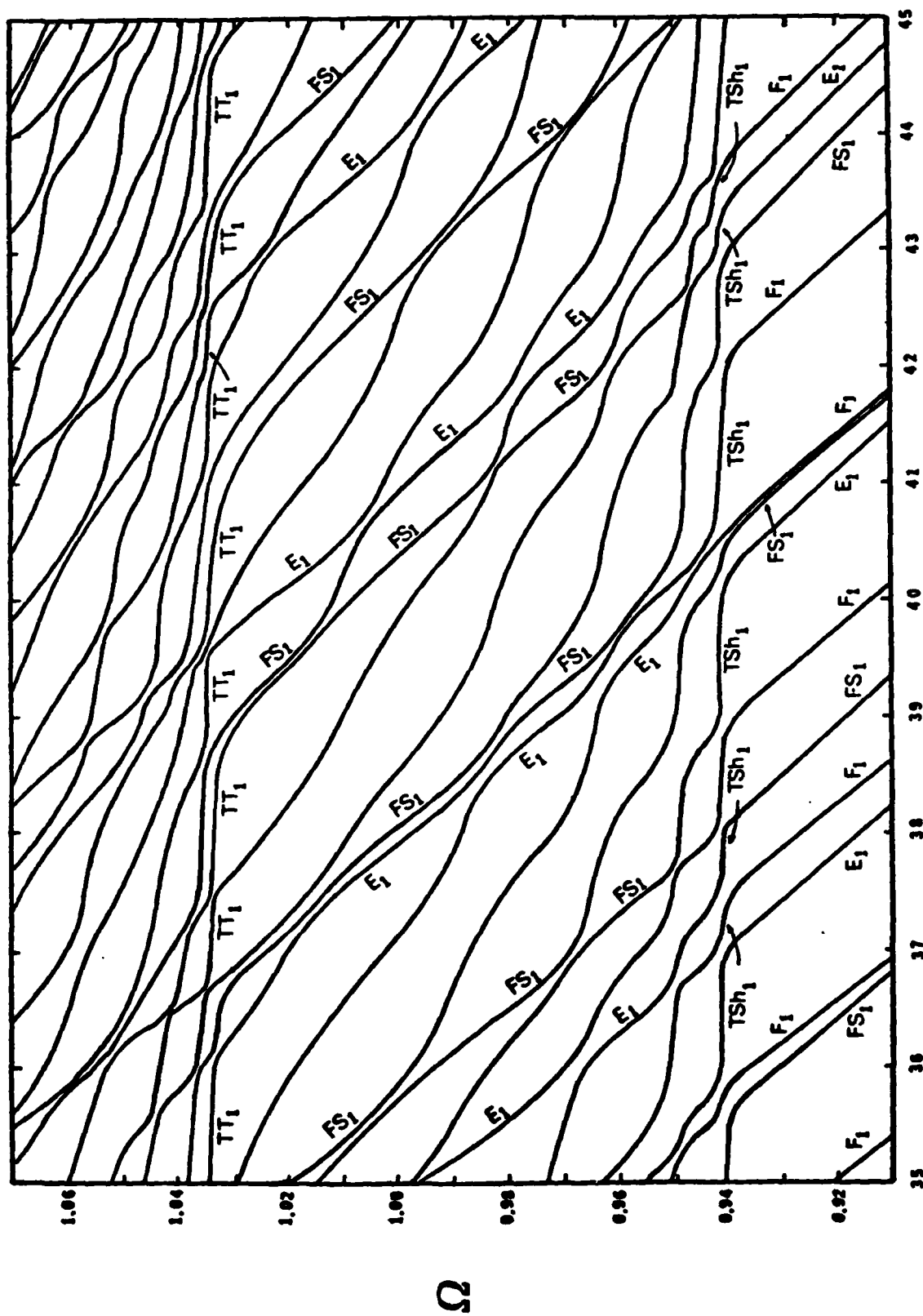
Fig. 5 Frequency spectra of SC-cut quartz plate for waves propagating in the $x_1$-direction $(35 \leq a/b \leq 45)$. (6 modes)
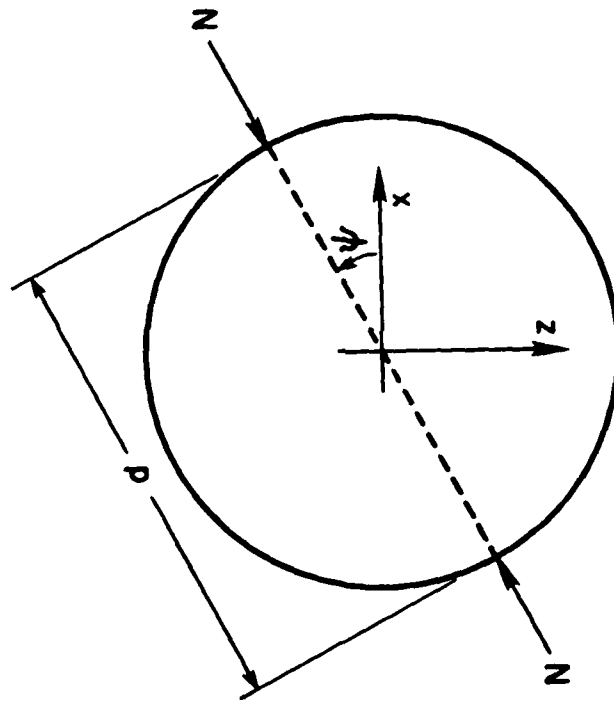
Fig. 6  A circular plate under diametral forces.
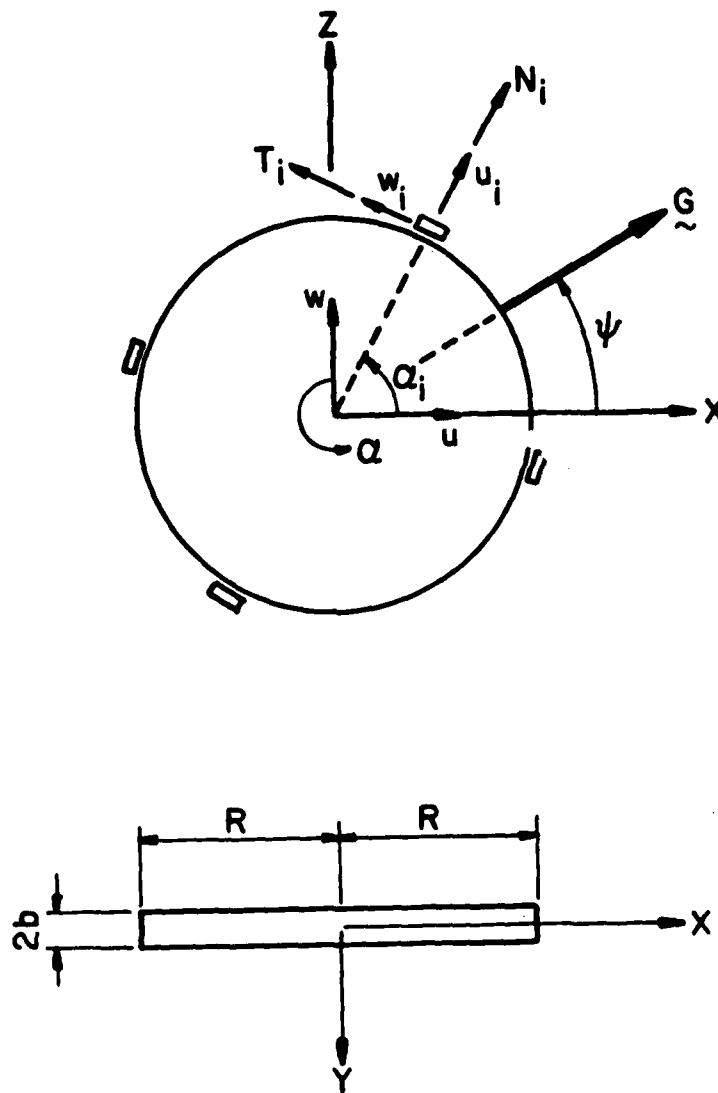
Fig. 7  A circular plate under body force  $\underset{\sim}{G}$.
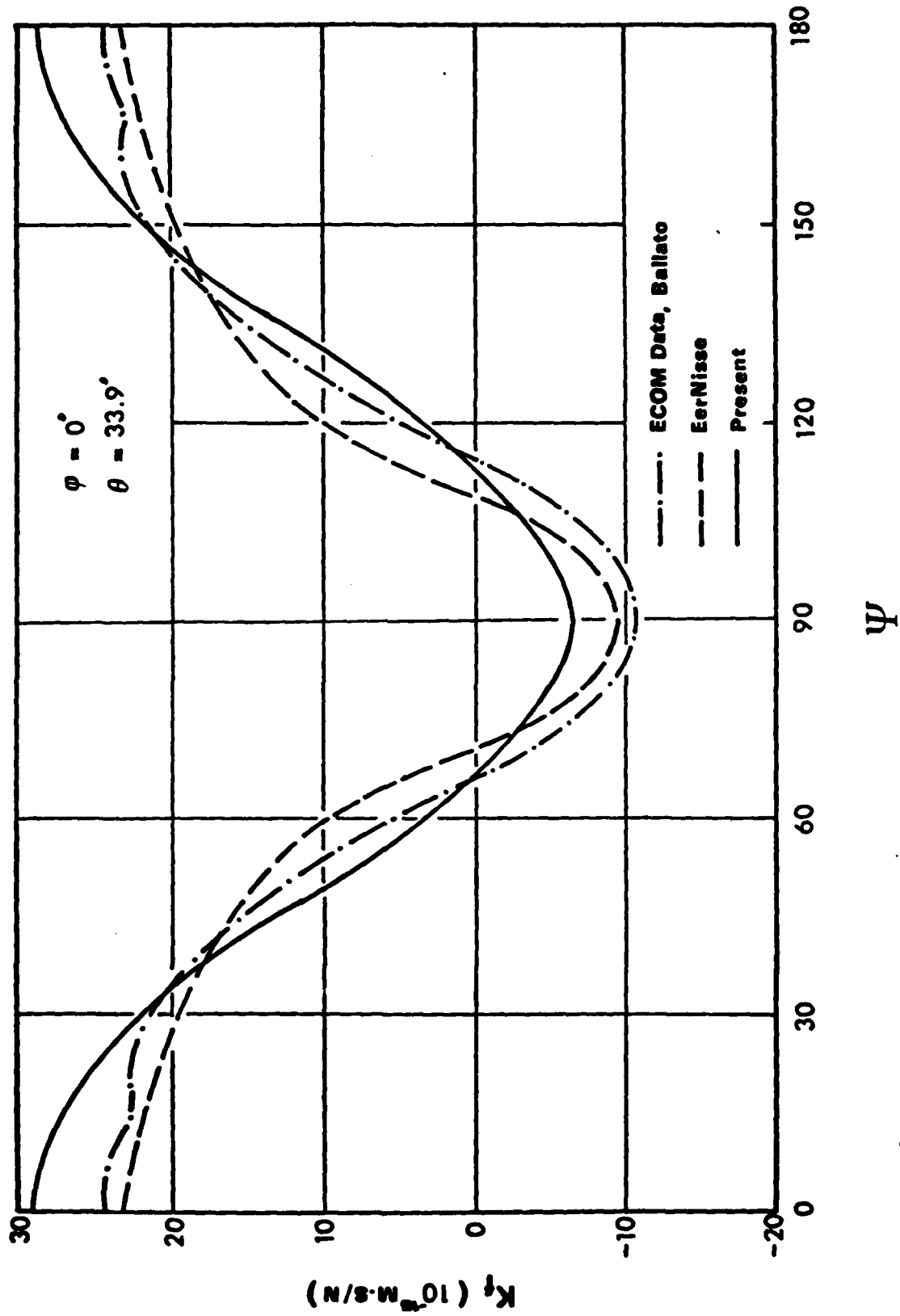
Fig. 8 Force sensitivity coefficient $K_f$ as a function of the azimuth angle $\psi$ of the pair of diametral forces, for AT-cut plate (yxℓ) 33.9°.
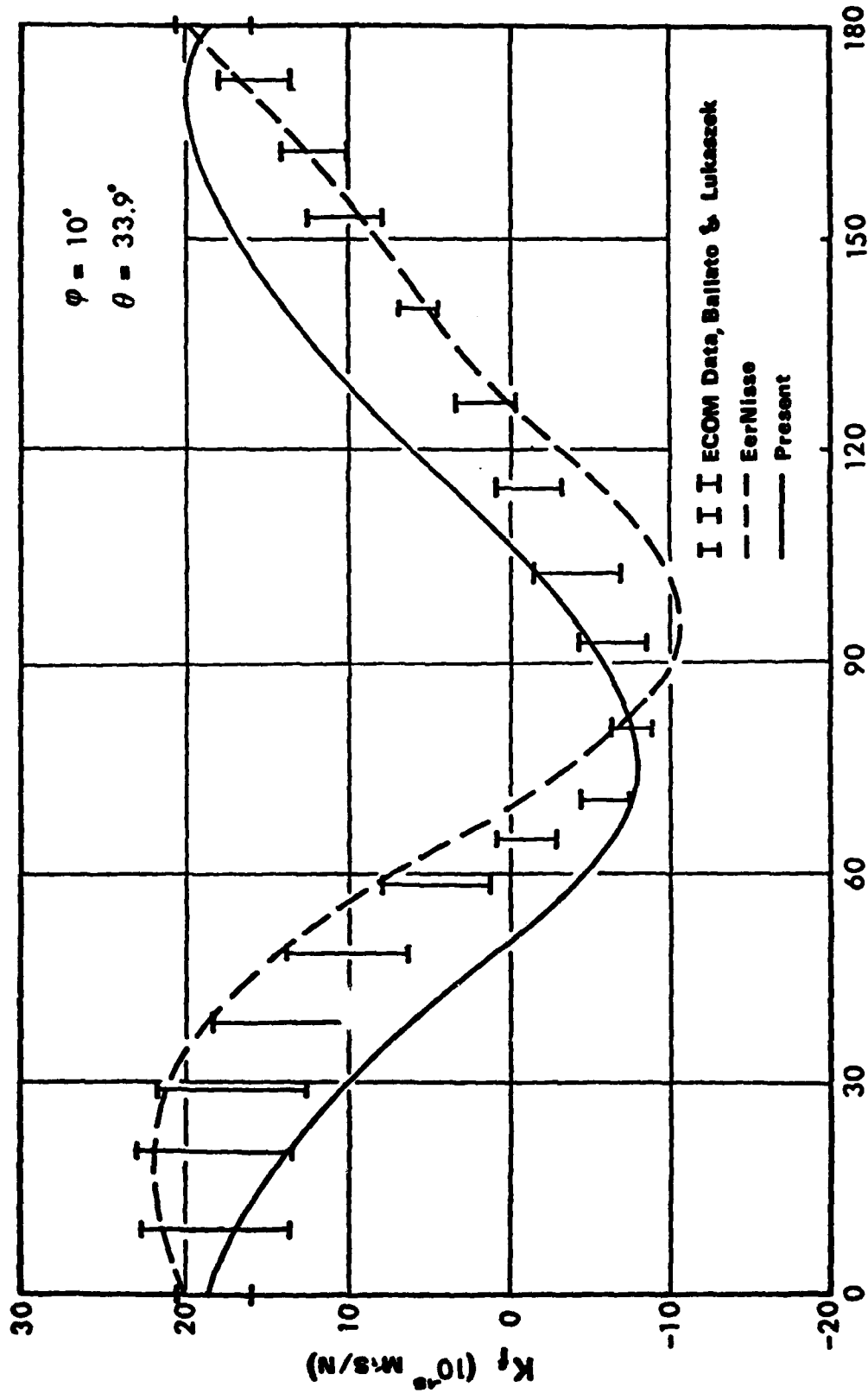
Fig. 9   $K_f$ vs. $\psi$ for quartz plate (yxwℓ) 10°/33.9°.
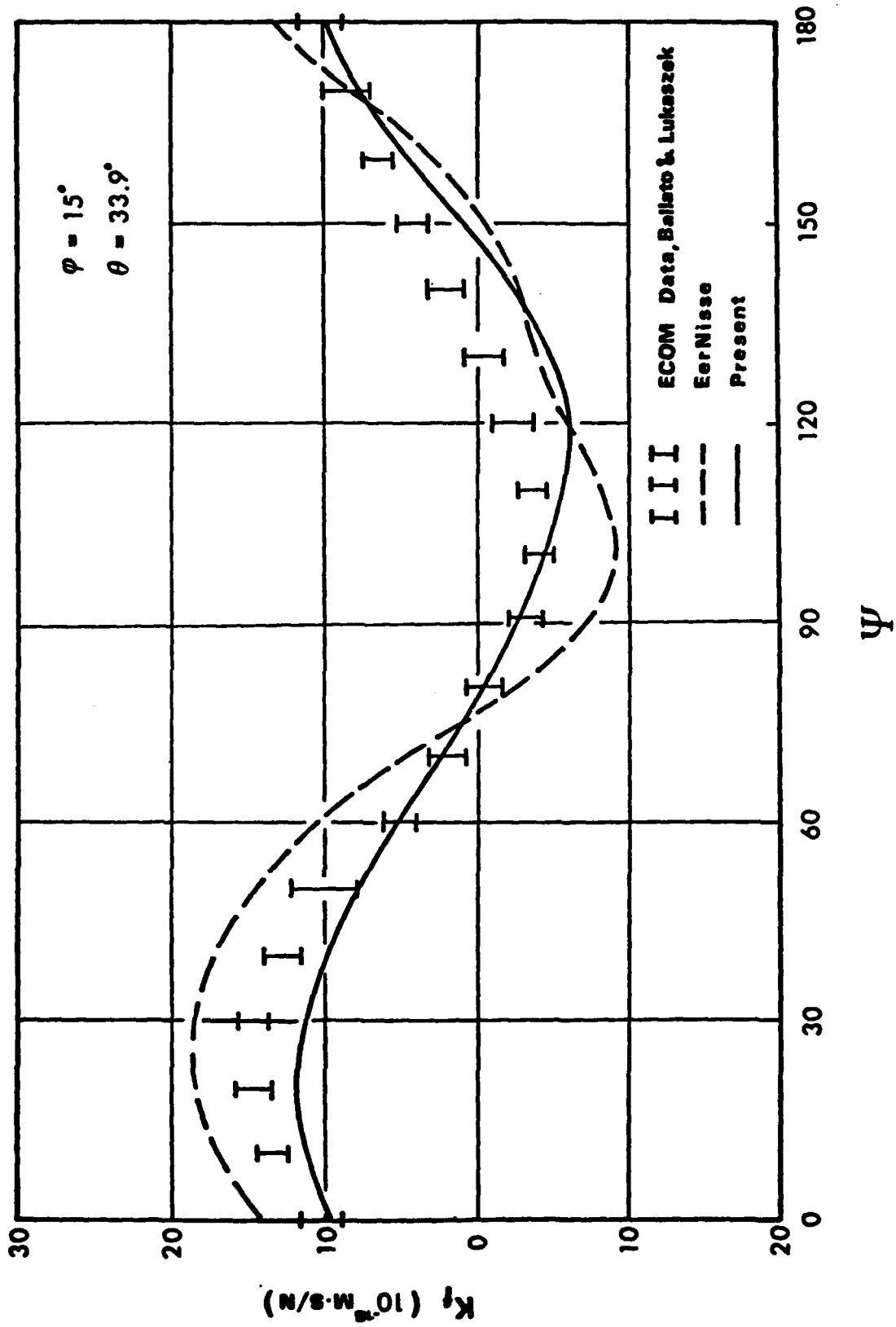
Fig. 10  $K_f$ vs. $\psi$ for FC-cut plate (yxwℓ) 15°/33.9°.
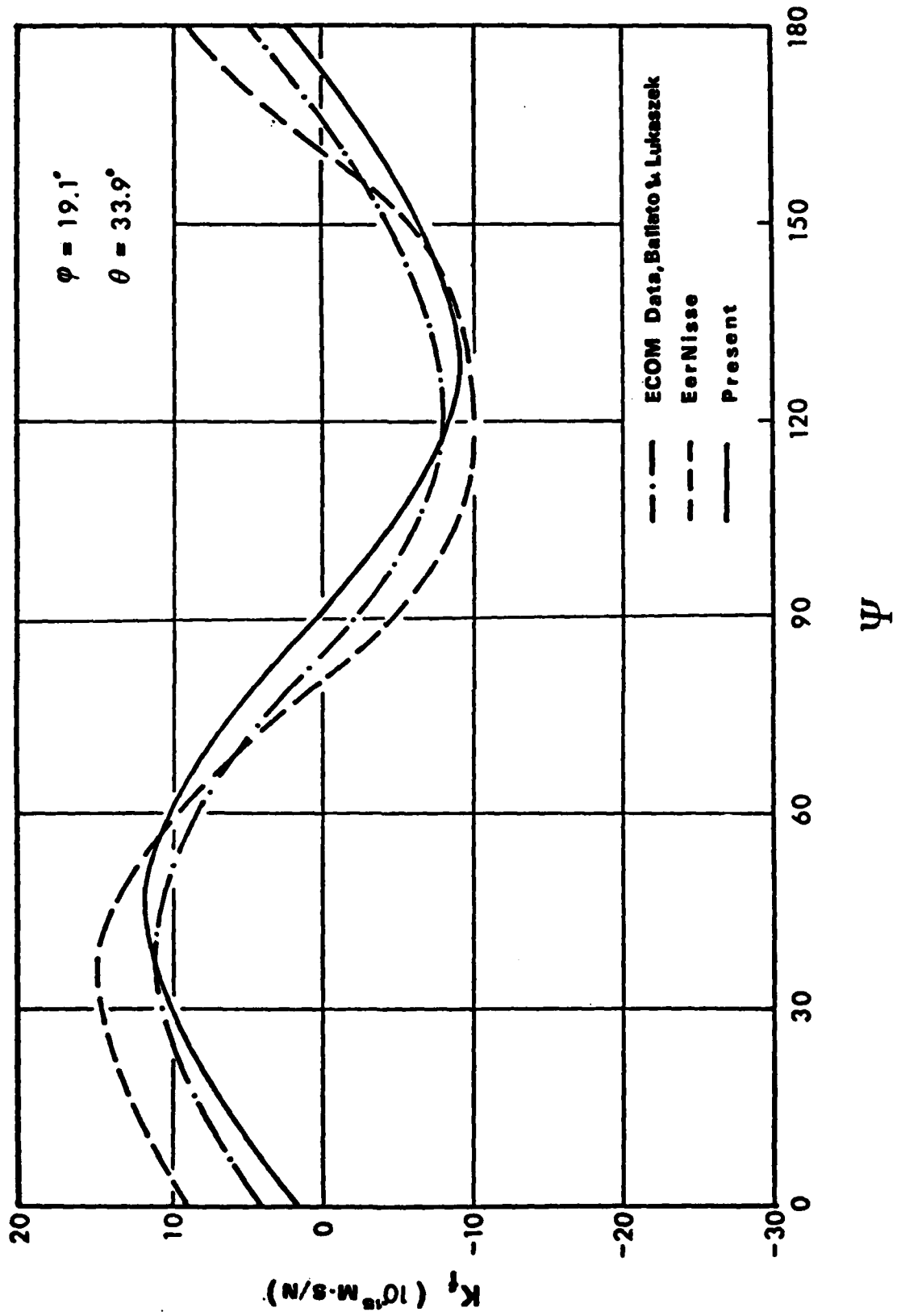
Fig. 11  $K_f$ vs. $\psi$ for IT-cut plate (yxwℓ) 19.1°/33.9°.
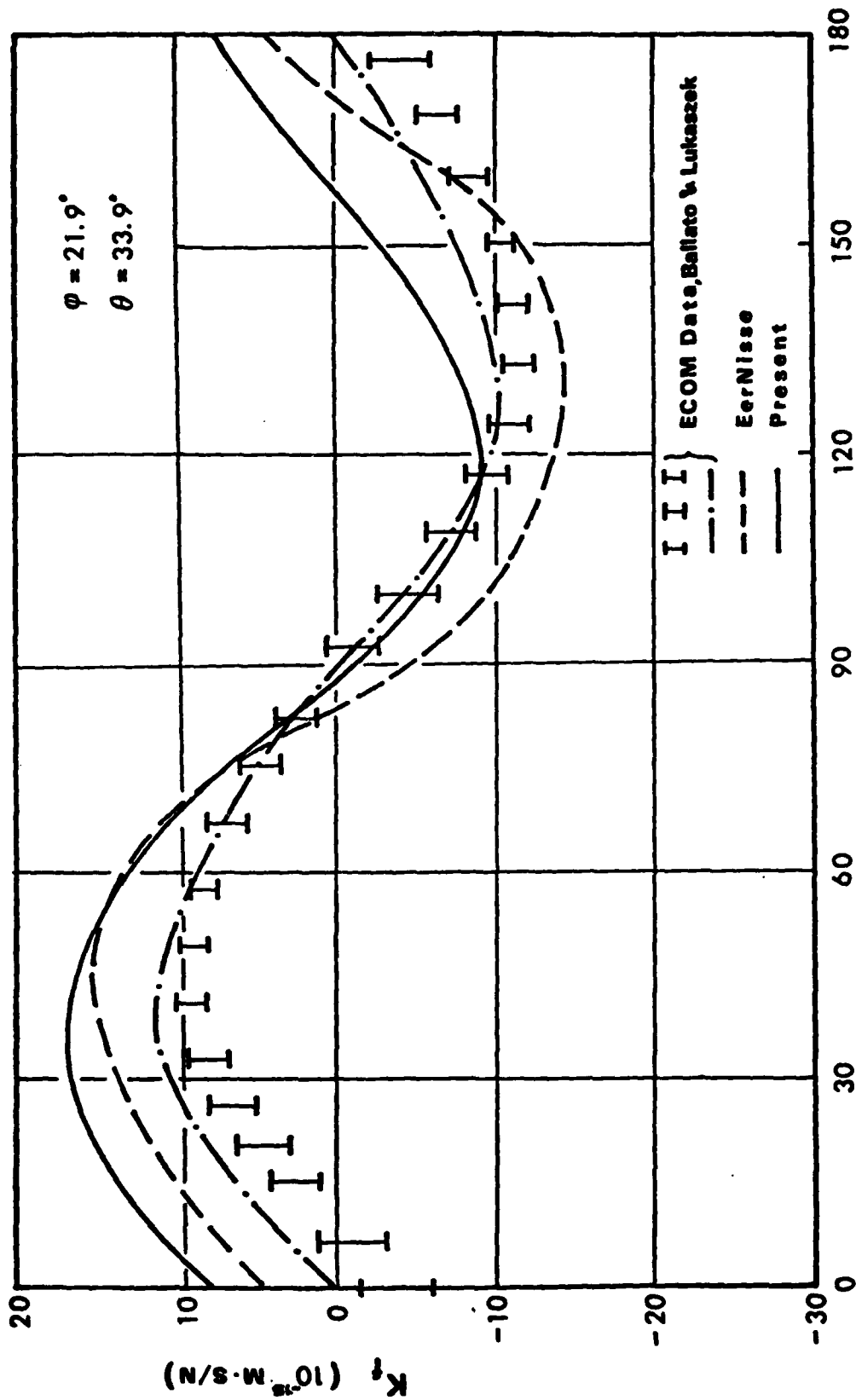
Fig. 12 $K_f$ vs. $\psi$ for SC-cut plate (yxwℓ) 21.9°/33.9°.
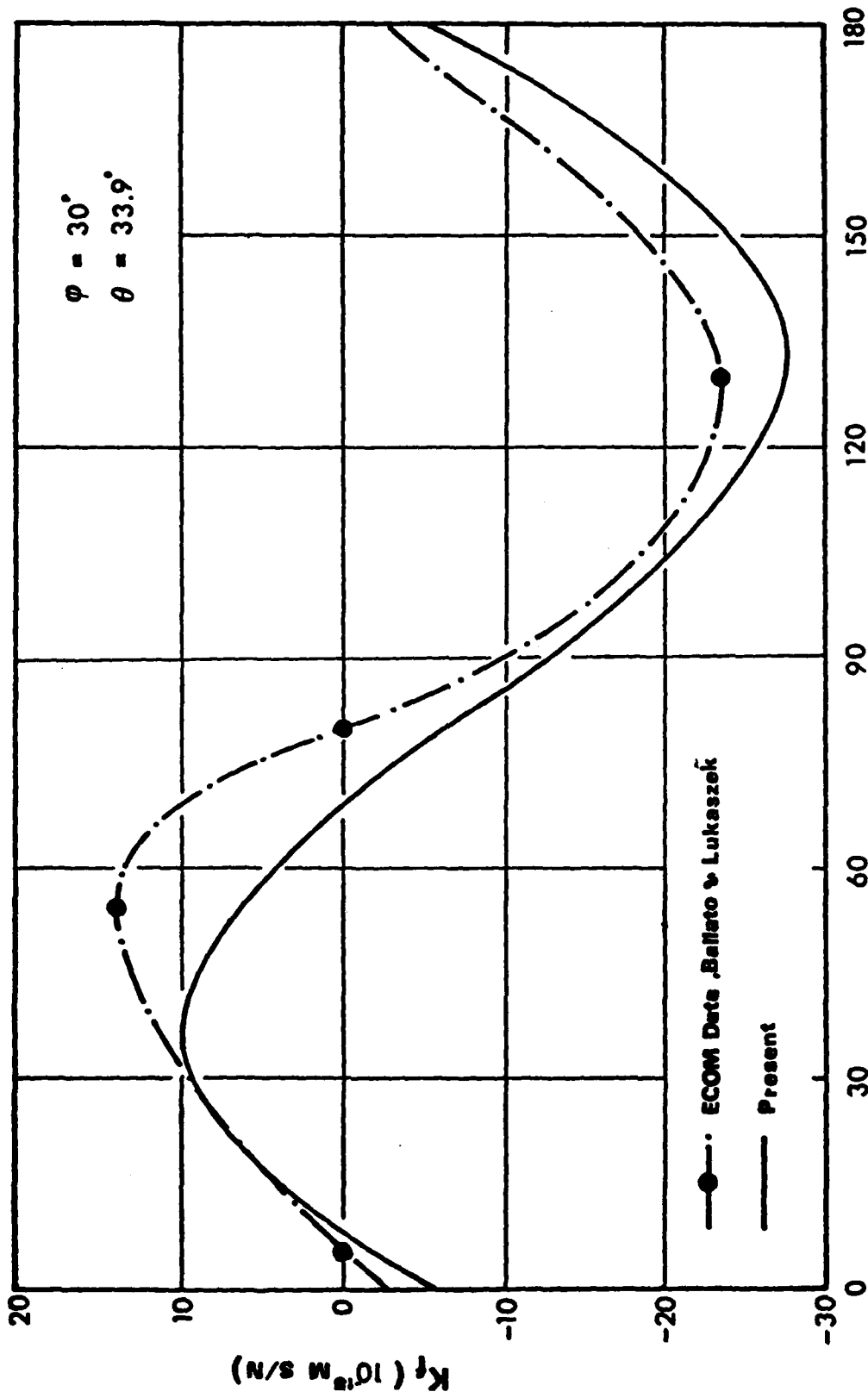
Fig. 13 $K_f$ vs. $\psi$ for Rotated-X-cut plate (yxwℓ) 30°/33.9°.
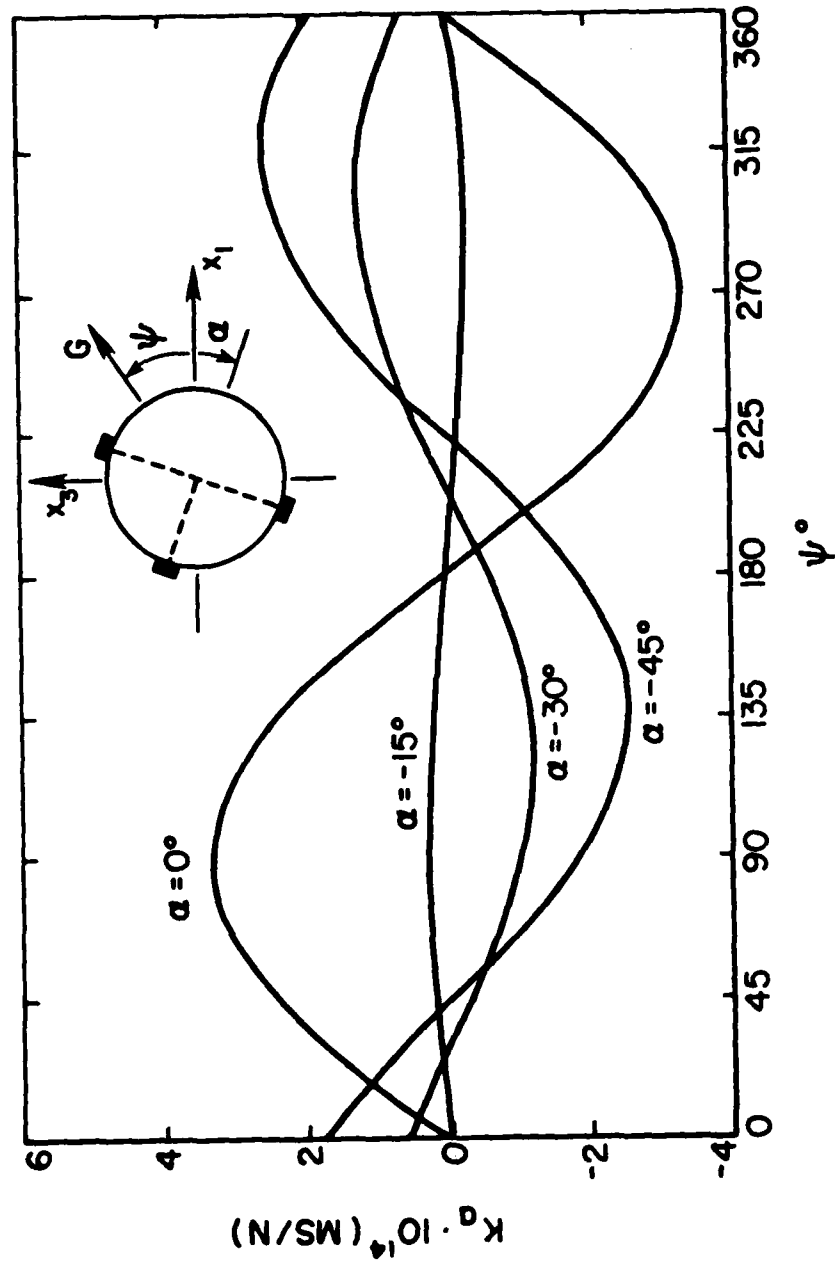
Fig. 14 Acceleration sensitivity coefficient $K_a$ as a function of the orientation of body force $\psi$, for SC-cut plate with "T" shaped mount.
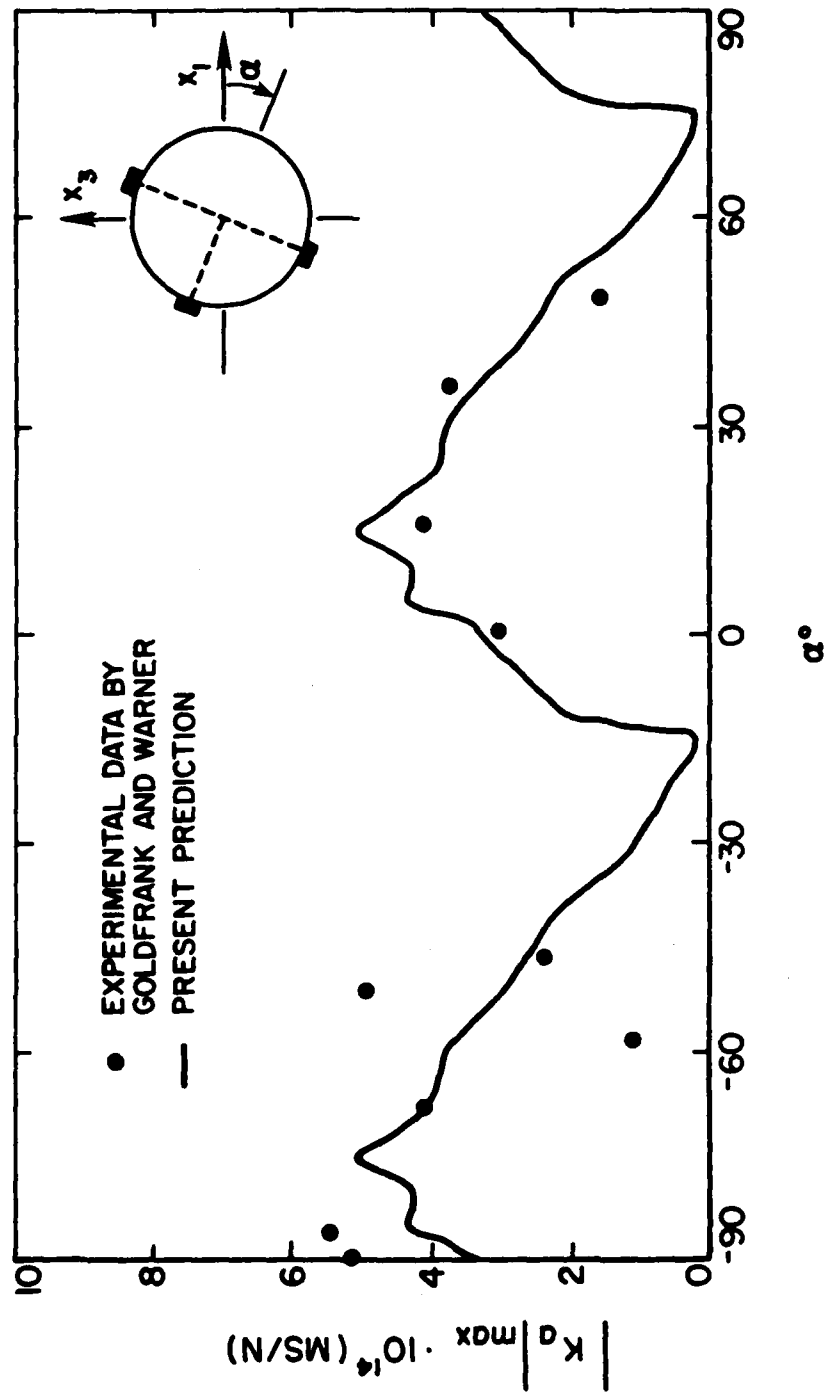
46



Fig. 15 $|K_a|_{max}$ vs. $\alpha$, for SC-cut plate with "T" shaped mount.
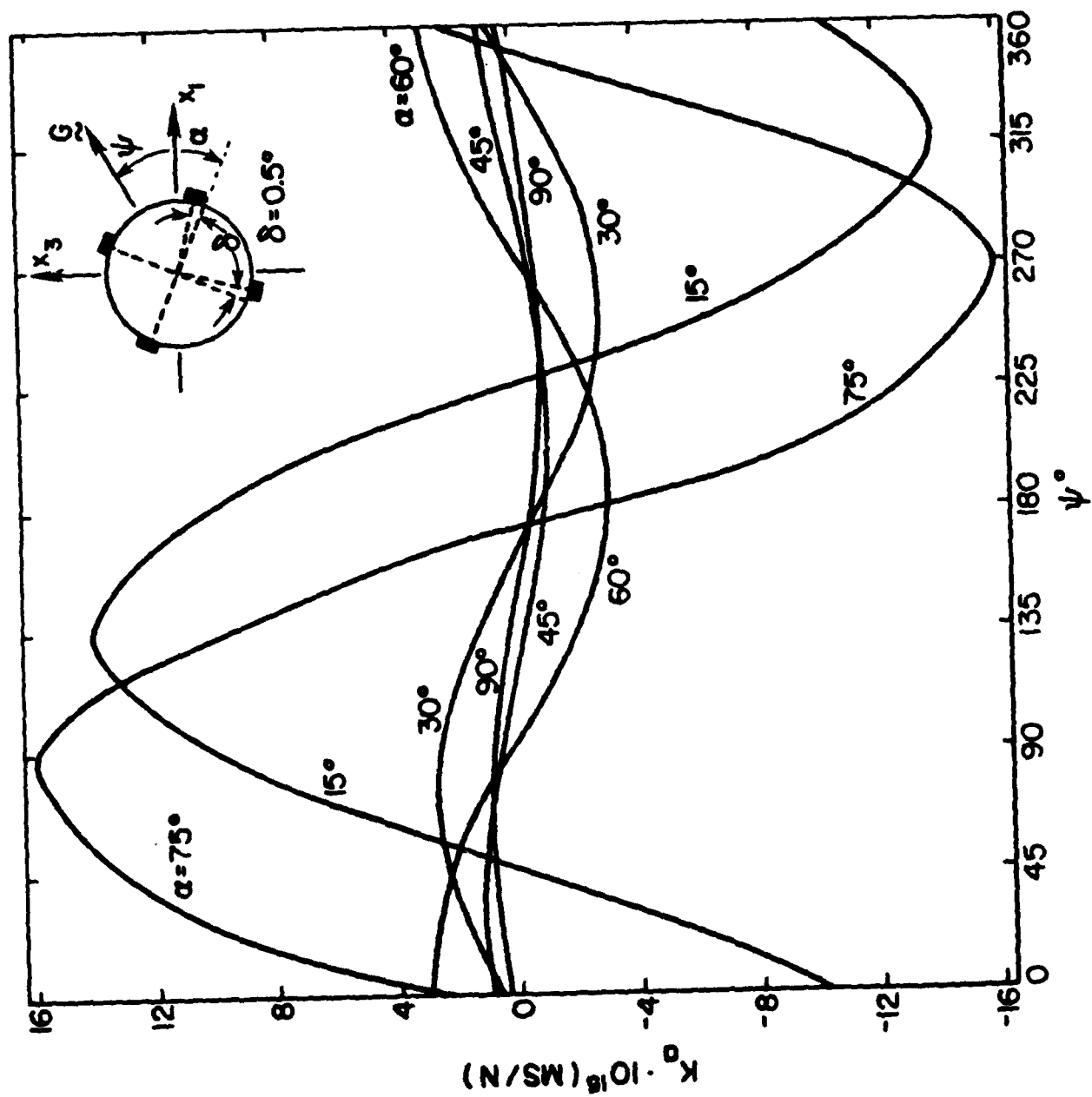
47



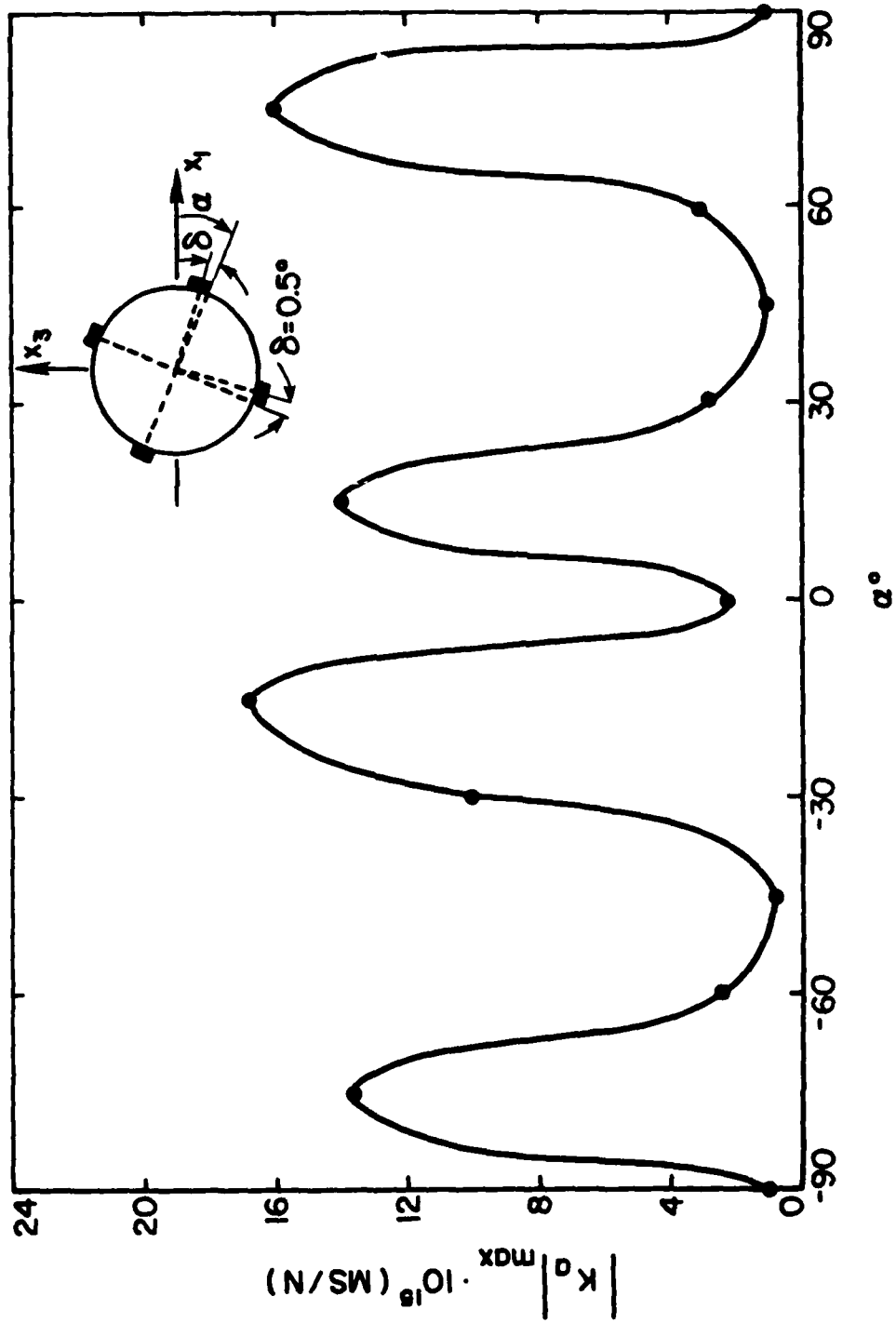Fig. 16   $K_a$ vs. $\psi$, for SC-cut plate with "+" shaped mount.

48



Fig. 17 $|K_a|_{max}$ vs. $\alpha$, for SC-cut plate with "+" shaped mount.

# FILM

6